Spherical collapse in Galileon models

Shabanov, Roman

Spherical collapse in Galileon models

THESIS

submitted in partial fulfillment of the
requirements for the degree of

BACHELOR OF SCIENCE
in
PHYSICS AND MATHEMATICS

Author :	R.O. Shabanov
Student ID :	s3109925
Supervisor :	Dr. A. Silvestri
	M. Pantiri
Second corrector :	Prof.dr. H.J. Hupkes

Leiden, The Netherlands, July 4, 2024

Spherical collapse in Galileon models

R.O. Shabanov

Instituut-Lorentz, Leiden University
P.O. Box 9500, 2300 RA Leiden, The Netherlands

July 4, 2024

Abstract

Galileon models form a class of models where an additional scalar field is added to the Lagrangian describing the general theory of relativity. The addition of the scalar field causes a wide array of phenomena within our universe to change. Among those phenomena are both the expansion of the universe and the formation of large scale structures. We will study how they are both changed within a subclass of the Galileon models, called the Galileon ghost condensate models. First, we explore the parameter space of the model to find the values that give rise to non-singular evolutions of the expansion of the universe. Then, we examine how the large scale structures would form within those universes. To do that we use the spherical collapse model, in which the evolution of a spherical overdensity is tracked. The spherical overdensity models how a relatively small perturbation leads to the formation of dark matter halos. We will show that the Galileon ghost condensate models still allow for a large degree of freedom within the spherical collapse, which would allow further research to constrain its parameter space.

Contents

Chapter 1

Introduction

In 1915 Albert Einstein introduced his theory of general relativity to the world. This theory is governed by the Einstein equations which describe how the spacetime is curved by the presence of mass and energy and how this curvature leads to gravity. But he quickly discovered that his theory predicted an expanding universe, which defied the common conception that the universe must be static. Wanting to rectify what he saw as a problem he introduced the cosmological constant into his equations.

Then in 1922 Russian physicist Alexander Friedmann found a solution of the Einstein equations which models an expanding universe for any value of the cosmological constant. At first, Einstein considered this solution to be unphysical, thinking that the universe must be static. But as Hubble made some observations which confirmed that the universe was expanding, Einstein had to concede that Friedmann's solutions were right [Bel12]. Furthermore, Einstein together with the Dutch physicist Willem de Sitter managed to slightly modify Friedmann's universe by removing the cosmological constant. Thereafter, Einstein, reportedly, called the cosmological constant his "biggest blunder" [Gam56].

This remained the main model in cosmology through almost the rest of the 20th century, until in 1998 two teams of astrophysicists independently discovered that the expansion rate of the universe was increasing [RFC+98, PAG+99]. As a consequence, the cosmological constant had to be reintroduced into the Einstein's equations. But the vacuum energy, which is the main theory for how this constant emerges, provides a theoretical value which differs from the observed value by around 60 orders of magnitude [JJKT15]. This lead to people searching for alternative explanations of dark energy, as the force driving the accelerating expansion of the universe is now called.

One such possible explanation is to introduce an additional scalar field to the Einstein's equations. In particular, if we require that the equations of motion contain at most second order derivatives of this scalar field, we get the Generalised Galileon model, also known as Horndeski gravity [Hor74]. Besides generalising many other theories with an additional scalar field, this model also acts as a low energy limit of most other theories of Modified Gravity [HS24].

To constrain the space of possible Generalised Galileon models, it is useful to look at how these models influence the development of large scale structures of the Universe. In particular, spherical collapse is the process through which small spherical overdensities in the early Universe evolved and later collapsed to form halos in the centre of which we now find the galaxies.

In Chapter 2 we shall first provide an overview of the theory of general relativity and cosmology. Afterwards we shall derive the spherical collapse model and briefly discuss how it behaves in unmodified gravity.

Chapter 3 first introduces the Galileon model in general. Then we will slowly narrow our focus to the two models we will study: covariant cubic Galileon and Galileon Ghost condensate. Along the way, we will explore what kind of modifications should be made to spherical collapse to accommodate those two models. Lastly, we will explore how the evolution of the universe changes due to the modifications to gravity.

Then, Chapter 4 will contain numerical simulations of the models we just discussed. First, the background evolution of the universe will be simulated with different initial conditions. Then, for some of those initial conditions we will simulate how the spherical collapse happens and compare that to spherical collapse in unmodified gravity.

Finally, in Chapter 5 we will discuss the results of the simulations and suggest some further areas of research.

Conventions

Einstein's summation notation will be used in this thesis. This means that whenever two indices, one upper and one lower, are repeated, then this implies a sum of all the values of the index. Furthermore, unless otherwise stated, Greek indices shall range over temporal and spatial components $\{0, 1, 2, 3\}$, while Latin indices range only over the spatial components $\{1, 2, 3\}$. Partial derivatives will sometimes be written using the symbol $\partial_i := \frac{\partial}{\partial x^i}$. Throughout the entirety of this thesis we will use units where $c = 1$.

Chapter 2

General Relativity

In 1915 Albert Einstein introduced his general theory of relativity. In it spacetime is described as a four-dimensional manifold whose curvature generates gravity. This curvature is governed by the Einstein equations in which the matter content of the universe is connected to the curvature. As gravity is the force that holds together the Universe at the large scales, it is general relativity that underlies modern cosmology.

2.1 Spacetime

In Newtonian mechanics we look at time and space as two entirely separate objects. But with the formulation of special relativity, Einstein found that space and time are intrinsically linked and should be considered as one object: spacetime. Later, mathematician Hermann Minkowski found that spacetime can be described as a four-dimensional space $\mathbb{R}^4$ on which the inner product is given by the matrix $\eta = \text{diag}(-1, 1, 1, 1)$, where the first basis vector is the time vector and the other three are standard basis vectors of the three-dimensional space. This space is called the Minkowski manifold, where a manifold is a space which locally resembles $\mathbb{R}^n$ for some dimension n.

In general relativity, though, we want spacetime to be able to curve and change. So, instead of η we will use a general metric $\mathbf{g}$ with components $g_{\mu\nu}$. This metric is a tensor field whose values depend both on the time and on the position. We will usually denote the components of the metric using the line element ds:

$$ds^2 = g_{\mu\nu} dx^\mu dx^\nu, \tag{2.1}$$

where we apply the Einstein summation notation. A metric must be symmetric $g_{\mu\nu} = g_{\nu\mu}$. So, instead of writing the off-diagonal components of the metric twice as in $g_{12}dx^1dx^2 + g_{21}dx^2dx^1$, we will write them as $2g_{12}dx^1dx^2$.

Spacetime must also locally resemble Minkowski space. Therefore, for every point p there must be some coordinates so that at that point $g_{\mu\nu}$ has the same components as η. Those coordinates are called normal coordinates centred at p. Furthermore, a metric must be non-degenerate $g := \det(\mathbf{g}) \neq 0$ and infinitely differentiable. Therefore, g must be continuous. It must also be negative in at least one point. As such, $g < 0$ on the entire spacetime. The non-degeneracy condition also ensures that $g_{\mu\nu}$ has an inverse, which we denote by $g^{\mu\nu}$.

Notice that even in Euclidean coordinates we have to add additional terms to the partial derivatives if we want to differentiate a vector in non-standard coordinates, such as the polar coordinates. But in a general manifold there are no standard coordinates, so to make a proper derivative we have to introduce additional terms in all coordinates. In this way, we can introduce a whole class of derivatives called the covariant derivatives. When working with manifolds with a metric there is a covariant derivative which is particularly useful: the Levi-Civita connection ∇_μ.

Just as with every covariant derivative, the Levi-Civita connection, when applied on a scalar field ϕ, gives a covector field given by the normal partial derivatives $\nabla_\mu\phi = \partial_\mu\phi$. However, when applied on a vector field v^ν it gives

$$\nabla_\mu v^\nu = \partial_\mu v^\nu + \Gamma^\nu_{\mu\lambda} v^\lambda, \tag{2.2}$$

where $\Gamma^\nu_{\mu\lambda}$ are called the Christoffel symbols and they are given by

$$\Gamma^\nu_{\mu\lambda} = \frac{1}{2} g^{\nu\rho}(\partial_\mu g_{\lambda\rho} + \partial_\lambda g_{\nu\rho} - \partial_\rho g_{\mu\lambda}). \tag{2.3}$$

For a covector field ω_ν this covariant derivative would give

$$\nabla_\mu \omega_\nu = \partial_\mu \omega_\nu - \Gamma^\lambda_{\mu\nu}\omega_\lambda, \tag{2.4}$$

while for a general tensor $T^{\nu_1\ldots\nu_k}_{\mu_1\ldots\mu_n}$ we would contract $\Gamma^\nu_{\mu\lambda}$ with each of the indices and then either add resulting term for the upper indices or subtract it for the lower indices [Car19, Eq. 3.17].

The property of the Levi-Civita connection that makes it special is $\nabla_\rho g_{\mu\nu} = 0$. This allows us to raise $\omega^\mu := g^{\mu\nu}\omega_\nu$ and lower $v_\mu := g_{\mu\nu}v^\nu$ the indices without the covariant derivative interfering. It also ensures that the

derivative of the inner product of two vectors $v^\mu u_\nu := g_{\mu\nu} v^\mu u^\nu$ acts as we would expect $\nabla_\rho(v^\mu u_\nu) = \nabla_\rho(v^\mu)u_\nu + v^\mu \nabla_\rho(u_\nu)$. Since we will only be using the Levi-Civita connection, we will call it simply the covariant derivative.

Using the Christoffel symbols we can also define the Riemann curvature tensor

$$R^\rho{}_{\sigma\mu\nu} = \partial_\mu \Gamma^\rho_{\nu\sigma} - \partial_\nu \Gamma^\rho_{\mu\sigma} + \Gamma^\rho_{\mu\lambda}\Gamma^\lambda_{\nu\sigma} - \Gamma^\rho_{\nu\lambda}\Gamma^\lambda_{\mu\sigma}. \tag{2.5}$$

This tensor represents the curvature of the spacetime. An intuitive explanation for how this expression is derived can be found in [Car19, Sec. 3.6].

We can then contract the Riemann curvature tensor to get the Ricci tensor $R_{\mu\nu} := R^\rho{}_{\mu\rho\nu}$. This tensor can be contracted once again to get the Ricci scalar $R = R^\mu_\mu$, also known as the scalar curvature. All other scalars formed through contractions of the Riemann tensor can be written as some multiple of the the Ricci scalar [Car19, p. 129]. So, we can think of it as an in some form unique scalar that characterises the curvature of spacetime.

2.2 Einstein Equation

To see what kind of equations govern the evolution of the metric $g_{\mu\nu}$ we will use the Lagrangian formulation of mechanics. Therein, we have the action S which is given by

$$S = \int \mathcal{L} dV_g \tag{2.6}$$

with $\mathcal{L}$ being the Lagrangian density and $dV_g = \sqrt{-g}d^4x$ being the pseudo-Riemannian volume form. This volume form ensures that the integral is coordinate independent. The principle of stationary action then says that the physical system must obey the equation $\delta S = 0$. For the metric $g_{\mu\nu}$ this means that $S[g_{\mu\nu} + \delta g_{\mu\nu}] - S[g_{\mu\nu}]$ must be equal to 0 to the first order in $\delta g_{\mu\nu}$.

We are using Lagrangian formulation, because it is easy to see whether an expression is coordinate invariant, as we would expect from any physical theory. The only requirement is for the Lagrangian to consist of only proper scalar functions. This allows us to easily modify the equations of GR and to introduce new fields, as we will do in Chapter 3.

As we saw in the previous section the Ricci scalar R is in some form the simplest scalar characterising the curvature of spacetime, as such we can try to set $\mathcal{L} = R$. This happens to be correct in the absence of matter. Our

universe, however, contains matter, so we also have to add the matter Lagrangian $\mathcal{L}_m$, whose precise form depends on the configuration of matter. In this way we get the Einstein-Hilbert action

$$S = \int \left[\frac{1}{2\kappa} R + \mathcal{L}_m \right] \sqrt{-g} d^4x. \tag{2.7}$$

Here we have also introduced the constant κ. This constant is needed to rectify the dimensions, as a Lagrangian density has the dimensions of energy per volume, while the Ricci scalar has the dimensions of inverse length squared. Note that we are working in units with $c = 1$, so time and length have the same units.

By applying the principle of stationary action, we get the Einstein field equation (EFE)

$$R_{\mu\nu} - \frac{1}{2} R g_{\mu\nu} = \kappa T_{\mu\nu}. \tag{2.8}$$

Here $T_{\mu\nu} := -\frac{2}{\sqrt{-g}} \frac{\delta S_m}{\delta g^{\mu\nu}}$ is the energy-momentum tensor, which can be obtained from $S_m = \int \mathcal{L}_m \sqrt{-g} dx^4$. The expression $R_{\mu\nu} - \frac{1}{2} R g_{\mu\nu}$ is often written as $G_{\mu\nu}$ and it is called the Einstein tensor.

By taking the non-relativistic limit of this equation and comparing to Newton's law of gravitation we can conclude that $\kappa = 8\pi G$ with G the gravitational constant [Car19, Sec. 4.2].

In addition, the Ricci tensor must satisfy the contracted Bianchi identity $\nabla^\mu R_{\mu\nu} = \frac{1}{2} \nabla_\nu R$ [Lee18, Prop. 7.18]. This identity can be rewritten as $\nabla^\mu G_{\mu\nu} = 0$. From this and the Einstein equation (2.8) we find the following expression:

$$\nabla^\mu T_{\mu\nu} = 0. \tag{2.9}$$

On a flat spacetime this gives the conservation of energy and conservation of momentum equations. This is why this identity is often called the conservation of energy equation or the continuity equation. In curved spacetime, however, the Christoffel symbols become non-zero, so energy and momentum are not globally conserved any more. But we still can find normal coordinates at each point so that the covariant derivative reduces to the normal derivative in that point. Therefore, the above equation implies local conservation of energy and momentum.

2.3 Cosmology

To study how the entire universe behaves, we assume that it is homogeneous and isotropic in space, i.e. the universe is the same at every point

and in every direction. This turns out to be true as long as we look at large enough scales. As the universe still evolves in time, the spacetime can be foliated into spacelike slices, where each slice represents the universe at one point in time. From the homogeneity and isotropy it also follows that each of the slices must be invariant under all possible spatial translations and rotations. We call those kind of spaces maximally symmetric spaces.

A maximally symmetric space can only have three possible geometries [Car19, Sec. 8.1]. It can be hyperbolic, spherical or flat. According to our best observations our universe is flat [AAA+20], therefore we shall only work with this case. The spacetime can then be neatly represented as $\mathbb{R} \times \mathbb{R}^3$, where $\mathbb{R}$ represents the time direction and $\mathbb{R}^3$ represents space, while the spacetime metric can be represented as

$$ds^2 = -dt^2 + a^2(t)\delta_{ij}dx^i dx^j, \tag{2.10}$$

where t is the time coordinate, x^i are the space coordinates, δ_{ij} is the three dimensional Euclidian metric and $a(t)$ is the scale factor. The scale factor encodes the expansion of the universe. Often, the scale factor is normalised through a change of coordinates so that it is equal to 1 in the present. This metric is know as the Friedmann-Lemaître-Robertson-Walker (FLRW) metric.

The coordinates used above are the comoving coordinates. They are the special coordinates in which the metric does not have any cross terms $dtdx^i$ and the coefficient of the time component dt does not depend on the spatial components.

For the universe to be homogeneous and isotropic, the matter and energy in the universe must also have the same properties. We can therefore model them as a perfect fluid with density ρ and pressure p. The energy-momentum tensor of perfect fluids is

$$T_{\mu\nu} = (\rho + p)U_\mu U_\nu + pg_{\mu\nu}, \tag{2.11}$$

where U_μ is the four-velocity of the fluid. A moving fluid is however not isotropic and therefore it won't create an isotropic metric. The fluid must thus be at rest in comoving coordinates, which means that

$$U^\mu = (1, 0, 0, 0). \tag{2.12}$$

This is exactly the reason why comoving coordinates are called that; the matter moves together with the coordinates.

By putting the FLRW metric and the energy-momentum tensor into the EFE (2.8) we get the two Friedmann equations

$$\left(\frac{\dot{a}}{a}\right)^2 = \frac{\kappa}{3}\rho \tag{2.13}$$

$$\frac{\ddot{a}}{a} = -\frac{\kappa}{6}(\rho + 3p). \tag{2.14}$$

Here the overdot represents a derivative with respect to time. Often the first of these two equations is simply called the Friedmann equation, while the other equation is called the second Friedmann equation. In most cases, Equation (2.13) alone is enough to solve for $a(t)$, which is why the second equation is rarely used.

Usually, we don't use $\dot{a}$ to characterise the rate of expansion of the universe, but rather we use the Hubble parameter

$$H := \frac{\dot{a}}{a}. \tag{2.15}$$

The value of the Hubble parameter right now is called the Hubble constant and it is denoted with H_0. According to current observations, H_0 is around 70 km/s/Mpc (pc stands for parsec, which is around 3 lightyears). Unfortunately, there are different ways of measuring this constant, and they give us two different values of 73 ± 1 and 67.3 ± 0.6 km/s/Mpc [RYM+22, AAA+20]. This discrepancy is called the Hubble tension and it forms one of the biggest unanswered questions in cosmology.

By rewriting the zero component of the continuity equation (2.9) we get

$$\frac{\dot{\rho}}{\rho} = -3(1 + w)H. \tag{2.16}$$

Here $w := \frac{p}{\rho}$ is the equation of state parameter. For most kinds of cosmological fluids w is constant. In that case, we can integrate the above equation with respect to a to get

$$\rho \propto a^{-3(1+w)}. \tag{2.17}$$

The two most well-known types of cosmological fluids are matter and radiation. Matter consists of nonrelativistic particles whose collisions with each other are negligible. As such, matter has practically zero pressure. It follows that the equation of state parameter of matter is equal to $w_M = 0$. According to Eq. 2.17, the energy density of matter goes as a^{-3}. This can

be explained by the amount of matter in the universe staying the same, but the volume of the universe increasing by a^3, which leads to a decrease in the number density of the particles.

Radiation consists of electromagnetic radiation, i.e. photons. Besides the decreasing number density, the energy of each photon also decreases by a factor of a^{-1} due to cosmological redshift. This leads to $\rho_R \propto a^{-4}$ and therefore $w_R = \frac{1}{3}$. Similar behaviour is also observed in massive particles moving at speeds close to the speed of light.

Matter can also be subdivided into two different parts: baryonic matter and dark matter. Baryonic matter is the usual visible matter, but it only constitutes around 15% of all matter. The rest is dark matter, which is called so because it does not interact with light. We have only observed it through gravitational effects and never directly. As such, we do not know what it is exactly, but the most favoured explanation says that it must be some form of cold dark matter (CDM). This means that dark matter consist of massive particles which move slowly. Furthermore, those particles must interact weakly with each other and with the rest of the universe through means other than gravity.

These two (or three) fluids alone are not enough to explain the behaviour of the universe. In particular, the second Friedmann equation (2.14) would then imply that the expansion of the universe is decelerating as ρ is always positive and p is always non-negative for any combination of radiation and matter. We know, however, from observations that the expansion of the universe is accelerating [RFC+98, PAG+99]. So, we have to add something to the model to rectify this problem. There are many different theories as to what could be added and all those theories we call by the umbrella term dark energy.

The most standard theory of dark energy is the addition of a third type of cosmological fluid: vacuum energy. Vacuum energy is an intrinsic energy of space, which stays constant at every point in space, even though the universe expands. This translates into $\rho_{DE} \propto a^0$. The equation of state of vacuum energy is then $p_{DE} = -\rho_{DE}$. The second Friedmann equation (2.14) then shows, as we wanted, that the expansion of the universe can accelerate as long as ρ_{DE} is large enough.

If we look at the expression of the energy-momentum tensor (2.11), then we see that vacuum energy contributes a term $p_{DE} g_{\mu\nu} = -\rho_{DE} g_{\mu\nu}$. It is customary to bring this term to the other side of the EFE (2.8):

$$G_{\mu\nu} + \Lambda g_{\mu\nu} = \kappa T_{\mu\nu}. \tag{2.18}$$

Here $\Lambda = \kappa \rho_{DE}$ is called the cosmological constant. This constant together with dark matter gives the name to Λ-CDM, also known as the standard

model of cosmology. Everything we have discussed in this section is part of this model.

Density parameters are often used instead of energy densities. They are defined by

$$\Omega_i := \frac{\kappa \rho_i}{3H^2}. \tag{2.19}$$

Here i represents the different kinds of cosmological fluids. Using these density parameters, we can rewrite the first Friedmann equation (2.13) in a simple form:

$$\Omega_m + \Omega_r + \Omega_{DE} = 1. \tag{2.20}$$

This suggests that the density parameters represent the fraction of energy in some region of space which comes from the corresponding fluid.

If we look at the history of our universe, we will find three different eras. First there was the radiation-dominated era, where $\Omega_r \approx 1$. But as radiation density decays the quickest, the Universe soon entered into the matter-dominated era, where $\Omega_r \approx 1$. Right now, we find ourselves at the point where dark energy starts to dominate over matter, as the matter energy density decays, while the dark energy density remains constant. The current values of the density parameters are $\Omega_{DE0} = 0.68 \pm 0.01$, $\Omega_{m0} = 0.32 \pm 0.01$ and $\Omega_{r0} \approx 10^{-4}$ [AAA+20]. In the future, the universe shall enter the dark energy dominated era. The evolution of the density parameters is shown in Fig. 2.1.

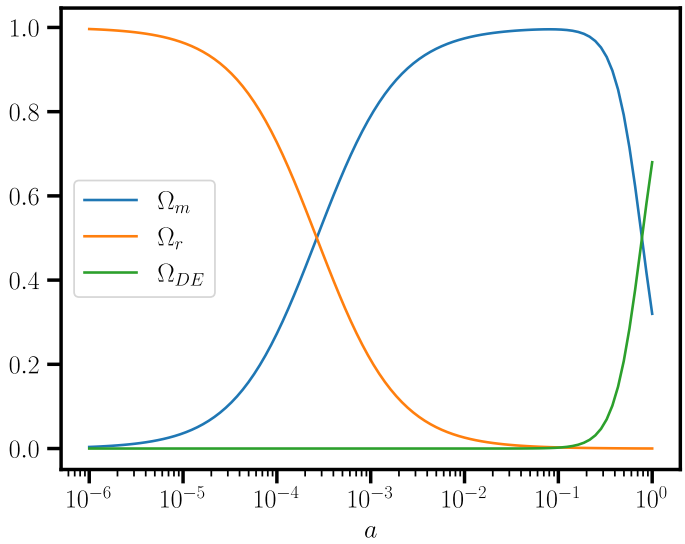

Figure 2.1: *Evolution of the density parameters in the Λ-CDM model as a function of the scale factor. The current values are set to* $\Omega_{DE0} = 0.68$, $\Omega_{m0} = 0.32$ *and* $\Omega_{r0} = 8.516 \cdot 10^{-5}$.

2.4 Perturbation Theory

Up until now we were working with the assumption that the universe is homogeneous. But even on the larger scales this is only approximately true. As such, we will divide the universe into homogeneous background, which was described before, and into perturbations of this background. So long as we look at large enough scales, we can assume that the perturbations are small relative to the background. In those cases, we can use linear perturbation theory, where we ignore second order and higher perturbation terms.

If we take the FLRW metric $g_{\mu\nu}$ as the background, then a general perturbed metric $g_{\mu\nu} + \delta g_{\mu\nu}$ can be written as follows:

$$ds^2 = -(1 + 2\hat{A})dt^2 + 2\hat{B}_i dt dx^i + a(t)^2(\delta_{ij} + h_{ij})dx^i dx^j. \tag{2.21}$$

Here, the 10 degrees of freedom of the perturbation are distributed between the single scalar degree of freedom $\hat{A}$, the three degrees of freedom of the vector $\hat{B}_i$ and the six degrees of freedom of the symmetric tensor h_{ij}. Furthermore, remember that δ_{ij} refers to the three dimensional Euclidean metric.

Note that those components of $\delta g_{\mu\nu}$ only act as tensors on the spatial slices and not on the entire spacetime. As such, we cannot use the covariant derivative associated with the full metric. Instead, we must use the covariant derivative associated with the metric δ_{ij} of the spatial slices, which we will denote as D_i. Note that we don't use the metric $\delta_{ij} + h_{ij}$ as the perturbations are defined with respect to the flat background space.

Using this, we can further decompose the perturbation $\delta g_{\mu\nu}$ into pure scalar, vector and tensor parts. The scalar $\hat{A}$ stays the same as $A = \hat{A}$. Then, we use Helmholtz decomposition on $\hat{B}_i$:

$$\hat{B}_i = D_i B + B_i. \tag{2.22}$$

Here B is a scalar and B_i is a divergence-free vector. The divergence-free condition $D^i B_i = 0$ ensures that this decomposition is unique. Furthermore, a divergence-free vector has two degrees of freedom and a scalar has one degree of freedom, which lets us see how the three degrees of freedom of $\hat{B}_i$ are divided.

Similarly, we can decompose the tensor h_{ij} as

$$h_{ij} = 2(C\delta_{ij} + D_{(i}D_{j)}E + 2D_{(i}E_{j)} + E_{ij}). \tag{2.23}$$

Here C and E are scalars, E_i is a divergence-free tensor and E_{ij} is a symmetric TT-tensor, which means that it is traceless ${E^i}_i = 0$ and transverse $D^i E_{ij} = 0$. This symmetric TT-tensor has two degrees of freedom.

Version of July 4, 2024– Created July 4, 2024 - 22:11

The above procedure is called the Scalar-Vector-Tensor (SVT) decomposition. An important feature of this decomposition is that it is unique. Furthermore, the scalar, vector and tensor parts do not mix at linear order. Therefore this decomposition allows us to treat those three parts separately from each other [Ste90]. Also note that in this case vector actually refers to divergence-free vectors and tensor refers to TT-tensors.

We have now defined four scalars A, B, C, E, two vectors B_i, E_i and a tensor E_{ij}. However, not all different combinations of those components give rise to different physical systems. After all, in GR coordinate transformations must leave the system unchanged. And as the spacetime is four-dimensional, the number of degrees of freedom of the perturbations must decrease by four.

Therefore, let us look at a coordinate transformation $x^\mu \mapsto \tilde{x}^\mu = x^\mu + \xi^\mu$, where ξ^μ is small. Coordinate independence then implies that the metric

$$d\tilde{s}^2 = -(1+2\hat{\tilde{A}})d\tilde{t}^2 + 2\hat{\tilde{B}}_i d\tilde{t}d\tilde{x}^i + a(\tilde{t})^2(\delta_{ij}+\tilde{h}_{ij})d\tilde{x}^i d\tilde{x}^j \tag{2.24}$$

has the same form as ds^2.

To find the transformation laws for the perturbation components, we use the SVT decomposition on ξ^μ. In that case the coordinate transformations can be written as $\tilde{t} = t + T$ and $\tilde{x}^i = x^i + D^i L + L^i$. This give us at linear order the following expressions

$$d\tilde{t} = dt + T'dt + D_i T dx^i, \tag{2.25}$$

$$d\tilde{x}^i = dx^i + D^i L dt + L'^i dt + D_j D^i L dx^j + D_j L^i dx^j, \tag{2.26}$$

$$a(\tilde{t}) = a(t) + a'(t)T. \tag{2.27}$$

Then, we put these equations into Eq. (2.24), while keeping everything at linear order. If we compare the result with Eq. (2.21), we get the following transformation laws

$$\tilde{A} = A - T', \quad \tilde{B} = B + T - a^2 L', \tilde{C} = C - HT, \quad \tilde{E} = E - L \tag{2.28}$$

for the scalar components,

$$\tilde{B}_i = B_i - a^2 L_i', \qquad \tilde{E}_i = E_i - L_i \tag{2.29}$$

for the vector components and

$$\tilde{E}_{ij} = E_{ij} \tag{2.30}$$

Version of July 4, 2024– Created July 4, 2024 - 22:11

for the tensor component.

We can now combine the two vector components to get a gauge-invariant quantity (a quantity that does not change under coordinate transformations):

$$\Phi_i = a^2 E_i' - B_i = a^2 \tilde{E}_i' - \tilde{B}_i. \tag{2.31}$$

Similarly, we can combine the scalar components:

$$\Psi = A - (a^2 E' - B)' = \tilde{A} - (a^2 \tilde{E}' - \tilde{B})', \tag{2.32}$$

$$\Phi = -C + H(a^2 E' - B) = -\tilde{C} + H(a^2 \tilde{E}' - \tilde{B}). \tag{2.33}$$

In this way, we have reduced the number of degrees of freedom to the two scalars Ψ, Φ, the two vector degrees of freedom Φ_i and the two tensor degrees of freedom E_{ij}, which gives us, just as expected, 6 degrees of freedom in total.

In the rest of this thesis only scalar perturbations will be needed. As such, we will set the other perturbations to zero. Furthermore, we will choose the coordinate frame such that $T = a^2 E' - B$ and $L = E$. In that case we have $B \to 0$, $E \to 0$ and the metric becomes

$$ds^2 = -(1 + 2\Psi)dt^2 + (1 - 2\Phi)\delta_{ij} dx^i dx^j. \tag{2.34}$$

This choice of a coordinate frame is called the Newtonian gauge, because in the Newtonian limit Ψ becomes the gravitational potential. Furthermore, if there is no anisotropic stress, i.e. if the pressure is the same in all directions at each point, then $\Phi = \Psi$ [Bau22, p. 217]. And all models we will consider do not have anisotropic stress. The Christoffel symbols and the Ricci scalar can be found in appendix A.1.

2.5 Spherical Collapse

Let us now look at a particular type of perturbation. We assume that in the early universe there is a spherical region of radius R, where there is a small overdensity $\delta\rho_m$ of dark matter. This overdensity has the same size in the entire spherical region, so that the overall density $\overline{\rho}_m + \delta\rho_m$ of matter has a top-hat profile. We will also assume that the collapse happens without introducing any kind of stresses. Then, the perturbation to the energy-momentum tensor can be expressed purely using the scalar $\delta\rho_m$. This allows us to only consider the scalar perturbations in the metric. So, we can use the perturbed metric in the Newtonian gauge (2.34).

We will also assume that the time derivatives of the metric and scalar field perturbations are negligible when compared to their spatial derivatives. This assumption is called quasi-static approximation (QSA). Furthermore, we will use the Newtonian slow speed limit, in which the four-velocity U^μ of the fluid as in Eq. (2.11) can be expressed as $(1, \mathbf{v})$. Here, $\mathbf{v}$ represents the three dimensional velocity of the fluid.

To get the equation which governs this spherical collapse, we will contract the continuity equation (2.9) with U_μ and with $g_{\mu\alpha} + U_\mu U_\alpha$. Note that we don't use here the entire energy momentum tensor, but only the matter part. Then, the contracted equations in the Newtonian limit become

$$\dot{\rho}_m + \nabla \cdot (\rho_m \mathbf{v}) + 3\rho_m H = 0, \tag{2.35}$$

$$\dot{\mathbf{v}} + (\mathbf{v} \cdot \nabla)\mathbf{v} + 2H\mathbf{v} + \frac{1}{a^2}\nabla\Phi = 0. \tag{2.36}$$

Here, we have also used that matter as a perfect fluid is pressureless. Also notice that both $\mathbf{v}$ and Φ are small and therefore their products can be ignored. These two equations are the continuity and Euler equations of pressureless fluids respectively in comoving coordinates.

Then, we can split the density ρ_m into the background density $\overline{\rho}_m$ and the overdensity $\delta\rho_m$. We also define the overdensity parameter $\delta = \delta\rho_m/\overline{\rho}_m$, so that $\rho_m = \overline{\rho}_m(1+\delta)$. Then, we put this into Eq. (2.35) and separate the background and the foreground parts to get the following equations

$$\dot{\overline{\rho}}_m + 3\overline{\rho}_m H = 0 \tag{2.37}$$

$$\dot{\delta} + (1+\delta)\nabla \cdot \mathbf{v} = 0. \tag{2.38}$$

Furthermore, we assume that during the spherical collapse there is no shear and that the overdensity does not rotate. In that case we can write [PWB10]

$$\nabla \cdot [(\mathbf{v} \cdot \nabla)\mathbf{v}] = \frac{1}{3}(\nabla \cdot \mathbf{v})^2. \tag{2.39}$$

Now, we take the divergence of the Euler equation (2.36), the time derivative of the foreground continuity equation (2.38) and combine them. This gives us the following equation

$$\ddot{\delta} + 2H\dot{\delta} - \frac{4}{3}\frac{\dot{\delta}^2}{1+\delta} = (1+\delta)\frac{\nabla^2\Phi}{a^2}. \tag{2.40}$$

We also assume that the overall mass of the spherical region with the overdensity is conserved during the entire collapse. This means that the

Version of July 4, 2024– Created July 4, 2024 - 22:11

following equation must be constant in time:

$$M = \frac{4\pi}{3} R^3 \rho_m (1+\delta) = \text{const.} \tag{2.41}$$

Then, we take the second time derivative of the equation above, combine it with Equations (2.37) and (2.40) and use that $\overline{\rho}_m \propto a^{-3}$ to finally get the equation governing the evolution of radius of the overdense region:

$$\frac{\ddot{R}}{R} = H^2 + \dot{H} - \frac{1}{3}\frac{\nabla^2 \Phi}{a^2}. \tag{2.42}$$

Notice that up until here we have not used the Einstein equations (2.8). As such, the equation above is independent of the specific Lagrangian for the metric. It is only now that we will specify that we are using standard GR. To do that, we take the 00-component of EFE (2.8) in the Newtonian limit and linearise the equation. By doing that, we get the Poisson equation:

$$\nabla^2 \Phi = 4\pi G a^2 \overline{\rho}_m \delta = \frac{\kappa}{2} a^2 \overline{\rho}_m \delta. \tag{2.43}$$

Here G is the gravitational constant.

By combining this with Eq. (2.42), we get

$$\frac{\ddot{R}}{R} = H^2 + \dot{H} - \frac{4\pi G}{3} a^2 \overline{\rho}_m \delta. \tag{2.44}$$

If we assume that we are in a matter dominated universe, then background matter density goes as $\overline{\rho}_m = \frac{1}{6\pi G}\frac{1}{t^2}$. In this case, the equation above has an analytic parametric solution

$$R = A(1-\cos\theta), \tag{2.45}$$

$$t = B(\theta - \sin\theta), \tag{2.46}$$

$$1+\delta = \frac{9}{2}\frac{(\theta-\sin\theta)^2}{(1-\cos\theta)^3}, \tag{2.47}$$

with an additional condition $A^3 = GMB^2$ [Bau22, sect. 5.4.1].

In this analytic solution we see that at first δ is small and so we can linearise its equation. We then get $\delta \propto t^{\frac{2}{3}} \propto a$. So, in the beginning the region with overdensity behaves like the rest of the universe. But, then it starts slowly to decouple and and grow less fast, until at $\theta = \pi$ the overdense region starts to shrink. Then, at $\theta = 2\pi$ the overdense region collapses into a singular point.

This model allows us to model the formation of dark matter halos, inside which the galaxies later form. In reality, this halo does not collapse into a single point. This does not happen, because the initial overdensity is not perfectly spherically symmetric and it has some angular momentum. As a result, the halo will virialise and settle into a state where the kinetic and potential energy balance each other according to the virial theorem

$$T = -\frac{1}{2}V. \tag{2.48}$$

Here T is the kinetic energy and V is the potential energy of the overdensity. But, as the time of virialisation is similar to the time of collapse, we will use the collapse to signify that a dark matter halo has formed.

Often, it is easier to use linear equations to analyse the formation of large scale structures. Gravitational collapse is, however, a non-linear process and so it cannot be described by linear equations. To find where collapse has happened, we can use the spherical collapse model. To do that we linearise the solution for δ and look at what happens at the time of collapse $t_{coll} = 2B\pi$. Using that we find the critical overdensity:

$$\delta_c = \frac{3}{20}\left(\frac{6t_{coll}}{B}\right)^{\frac{2}{3}} = \frac{3}{20}(12\pi)^{\frac{2}{3}} \approx 1.69. \tag{2.49}$$

Then when using the linear equations, it is assumed that a halo has formed, wherever the overdensity has reached the critical value.

The critical overdensity can, for example, be used to calculate the halo mass function using the Press-Schechter theory [Bau22, sect. 5.4.4]. This halo mass function gives the relative abundance of halos with a certain mass. And as halo mass function can also be calculated from observations, we can compare different models using the halo mass function.

Version of July 4, 2024– Created July 4, 2024 - 22:11

Chapter 3

Galileon Model

The usual way to explain dark energy is to add a cosmological constant Λ to the Einstein Field Equations as in Eq. (2.18). This constant represents vacuum energy, i.e. energy present even in vacuum. It arises due to the fact that quantum fields cannot have zero energy [RZ02]. A conservative calculation shows that $\Lambda_{\text{theory}} \approx 10^{-60} M_{pl}^4$ in Planck units, where $M_{pl} := (8\pi G)^{-1/2}$ is the Planck mass. However, the observed value is $\Lambda_{\text{obs}} \approx 10^{-120} M_{pl}^4$ which is 60 orders of magnitude smaller than the calculated value [JJKT15]. This discrepancy is called the cosmological constant problem or the vacuum catastrophe. This leads us to consider other theories of dark energy. In particular, those that work by modifying the way gravity works.

In this chapter, we will present Horndeski gravity, which is a theory of modified gravity where you add an additional scalar field φ while ensuring that the equations of motion remain second order. Then, we will focus on two particular models, called covariant cubic Galileon and the Galileon ghost condensate models. In particular, we will explore how those two models change the way that the spherical collapse happens. To do that we will also have to look at how they affect the evolution of the size of the universe.

3.1 Horndeski Gravity

Horndeski gravity, also known as generalised Galileon model, is the most general way to add a scalar field φ to the Einstein-Hilbert action so that the resulting equations of motion do not contain derivatives of the third or higher order. One way to look at the scalar field is that it represents an

additional particle which is coupled to the gravitational field. However, we can also treat Horndeski gravity as a low-energy effective action of gravity which characterizes the expanding FLRW universe and thus also dark energy [HS24]. This interpretation shows why studying Horndeski theory is much more useful than the literal interpretation of φ as a particle would suggest.

The Horndeski action is given by

$$S = \int d^4x\sqrt{-g}\left[\sum_{i=2}^{5}\mathcal{L}_i + \frac{1}{2\kappa}R + \mathcal{L}_m\right], \tag{3.1}$$

with

$$\begin{aligned}
\mathcal{L}_2 &= G_2(\varphi, X)\\
\mathcal{L}_3 &= G_3(\varphi, X)\Box\varphi\\
\mathcal{L}_4 &= G_4(\varphi, X)R + G_{4X}\left[(\Box\varphi)^2 - (\nabla_\mu\nabla_\nu\varphi)^2\right]\\
\mathcal{L}_5 &= G_5(\varphi, X)G_{\mu\nu}\nabla^\mu\nabla^\nu\varphi - \frac{1}{6}G_{5X}\left[(\Box\varphi)^3 - 3\Box\varphi(\nabla_\mu\nabla_\nu\varphi)^2\right.\\
&\quad \left.+2(\nabla^\mu\nabla_\nu\varphi)(\nabla^\nu\nabla_\rho\varphi)(\nabla^\rho\nabla_\mu\varphi)\right].
\end{aligned} \tag{3.2}$$

Here $X := \nabla^\mu\varphi\nabla_\mu\varphi$ is the kinetic term of the scalar field, $G_{\mu\nu}$ is the Einstein tensor and $G_i(\phi, X)$ are free functions of the scalar field and the kinetic term. We also use the notation $\Box\varphi := \nabla^\mu\nabla_\mu\varphi$, $(\nabla_\mu\nabla_\nu\varphi)^2 := (\nabla^\mu\nabla^\nu\varphi)(\nabla_\mu\nabla_\nu\varphi)$ and $G_{iX} := \partial G_i/\partial X$.

The free functions G_i can be combined into the four alpha parameters α_K, α_B, α_M and α_T, which are functions of time. Together with the Hubble parameter H and the current values of the density parameters Ω_i, they completely determine the behaviour of Horndeski gravity in linear perturbation theory as long as $\dot{\varphi} \neq 0$. The precise expression for these parameters can be found in [BS14].

Unlike the free functions G_i, the alpha parameters can be given a physical interpretation:

- α_K is the kineticity parameter. It roughly corresponds to the kinetic energy of the scalar perturbations. It has contributions from all four free functions G_i.

- α_B is the braiding parameter. It signifies the mixing of the kinetic terms of the scalar with the kinetic terms of the metric. It has contributions from G_3, G_4 and G_5.

- α_M is the Planck mass run rate. It can be seen as the rate of change of the Planck mass M_{pl} and hence the gravitational constant G. Anisotropic stress is introduced by this parameter. It has contributions from G_4 and G_5.
- α_T is the tensor speed excess. It represents the deviation of the speed of gravitational waves from the speed of light. Anisotropic stress is introduced by this parameter. It has contributions from G_4 and G_5.

3.2 Generalised Cubic Galileon

2017 saw the first detection of a neutron star merger using both gravitational waves and electromagnetic detectors. This event confirmed that the speed of gravitational waves is equal to the speed of light to within a factor of 10^{-15} [LVFI17]. It is, therefore, reasonable to assume that α_T is equal to zero.

Then, the definition of α_T given in [BS14] implies that

$$2G_{4X} - 2G_{5\varphi} - (\ddot{\varphi} - \dot{\varphi}H)G_{5X} = 0. \tag{3.3}$$

Here $G_{5\varphi} := \partial G_i/\partial\varphi$. Note that G_i do not contain second order derivatives of φ, therefore G_{5X} must be zero and $G_{4X} = G_{5\varphi}$.

However, we will only look at shift-symmetric models, i.e. the models whose G_i functions do not explicitly depend on φ. They are called that, because their Lagrangian does not change under a shift of the scalar field $\varphi \to \varphi + c$ with constant c. This leads us to set G_4 and G_5 to zero.

We are now only left with the $G_2(X)$ and $G_3(X)$ terms. This also implies that $\alpha_M = 0$, which means that there is no anisotropic stress introduced by the modification to gravity. Therefore, $\Psi = \Phi$ still holds as long as the stress-energy tensor T^{ij} does not introduce any anisotropic stress.

These assumptions allow us to simplify the action (3.1) to

$$S = \int d^4x\sqrt{-g}\left[G_2(X) + G_3(X)\Box\varphi + \frac{1}{2\kappa}R + \mathcal{L}_m\right]. \tag{3.4}$$

This action represents the shift-symmetric generalised cubic Galileon models.

By varying this action with respect to the metric we get the modified Einstein field equations:

$$\begin{aligned} &G_{2X}\nabla_\mu\varphi\nabla_\nu\varphi - \frac{1}{2}G_2 g_{\mu\nu} + G_{3X}\Box\varphi\nabla_\mu\varphi\nabla_\nu\varphi \\ &\quad -\nabla_{(\mu}G_3\nabla_{\nu)}\varphi + \frac{1}{2}g_{\mu\nu}\nabla^\rho G_3\nabla_\rho\varphi + \frac{1}{2\kappa}G_{\mu\nu} = \frac{1}{2}T_{\mu\nu}, \end{aligned} \tag{3.5}$$

while by varying the action with respect to the scalar field we get the equation of motion for the scalar field:

$$\nabla^\mu(2G_{2X}\nabla_\mu\varphi + 2G_{3X}\Box\varphi\nabla_\mu\varphi - G_{3X}\nabla_\mu X) = 0. \tag{3.6}$$

We have already seen that two alpha parameters α_M, α_T are equal to 0 in this model. The other two alpha parameters are given by

$$H^2M_{pl}^2\alpha_K = 2X(G_{2X} + 2XG_{2XX}) - 12\dot{\varphi}XH(G_{3XX}), \tag{3.7}$$

$$HM_{pl}^2\alpha_B = \dot{\varphi}XG_{3X}. \tag{3.8}$$

Furthermore, the speed of sound c_s of the scalar perturbations of φ is given by

$$\alpha c_s^2 = -2(1+\alpha_B)\left(\frac{H'}{H} + \alpha_B\right) - 2\alpha_B' - 3\Omega_m - 4\Omega_r, \tag{3.9}$$

where prime refers to the derivative with respect to the e-fold time $\ln a$, $\Omega_i := \rho_i/(3M_{pl}^2H^2)$ are the matter and radiation density parameters for $i = m, r$ respectively and $\alpha := \alpha_K + 6\alpha_B^2$ [AFPS24].

At the larger scales, there are many unknowns about how gravity works, which gives us the freedom to modify it. However, we do not have the same amount of freedom within the Solar System, considering how well we have tested gravity at these scales [Uza11]. As such, all theories of modified gravity must reduce to ordinary general relativity at the scale of a solar system. In particular, we want to get the Poisson equation (2.43) in the Newtonian limit.

To test when this constraint holds in generalised cubic Galileon models, we will assume that there is a spherical mass M of radius R_M. This mass represents the Sun in our solar system. Furthermore, we will divide the matter density into the background density $\overline{\rho}_m$ and the perturbation $\overline{\rho}_m(t)\delta(t,\mathbf{x})$ just as we did in Section 2.5. Similarly, we will separate the scalar field $\varphi(t,\mathbf{x}) = \overline{\varphi}(t) + \delta\varphi(t,\mathbf{x})$.

Now, we expand equations (3.5) and (3.6) to the second order around the perturbations. We will also assume that the gravitational potential Φ and its first order spatial derivatives are negligible compared to its second order spatial derivatives. Then, by using the quasi-static approximation the two equations become

$$\frac{\nabla^2\Phi}{a^2} = \frac{\overline{\rho}_m\delta}{2M_{pl}^2} + \alpha_BH\frac{\nabla^2\chi}{a^2}, \tag{3.10}$$

$$\frac{\nabla^2\chi}{a^2} + \lambda^2\left[\frac{(\nabla_i\nabla_j\chi)^2}{a^4} - \frac{(\nabla^2\chi)^2}{a^4}\right] = -\frac{\lambda^2}{2M_{pl}^2}\overline{\rho}_m\delta. \tag{3.11}$$

Here $\chi := \delta\varphi/\dot{\bar{\varphi}}$ is an auxiliary field, $(\nabla_i\nabla_j\chi)^2 := (\nabla^i\nabla^j\chi)(\nabla_i\nabla_j\chi)$ is calculated using the Euclidean metric and

$$\lambda^2 := -\frac{2\alpha_B}{H\alpha c_s^2}. \tag{3.12}$$

As the matter distribution is spherically symmetric, we can also assume that the scalar field has the same symmetry. We use this assumption to write Eq. (3.11) purely in terms of the radial distance r, then we multiply it by a^4r^2 and integrate it with respect to r to get

$$a^2r^2\frac{\mathrm{d}\chi}{\mathrm{d}r} - 2\lambda^2 r\left(\frac{\mathrm{d}\chi}{\mathrm{d}r}\right)^2 = -a^4\lambda^2 Gm(r), \tag{3.13}$$

where

$$m(r) := 4\pi\int_0^r r'^2\bar{\rho}_m\delta(r')dr' \tag{3.14}$$

is the mass of the overdensity in the spherical region with radius r whose centre coincides with the centre of the mass M.

The above equation can be solved algebraically for $\frac{\mathrm{d}\chi}{\mathrm{d}r}$:

$$\frac{\mathrm{d}\chi}{\mathrm{d}r} = \frac{a^2r}{4\lambda^2}\left(1 - \sqrt{1 + \frac{r_V^3}{r^3}}\right). \tag{3.15}$$

Here $r_V^3 := 8\lambda^4 Gm$ is called the Vainshtein radius. Notice that $m(r) = M$ for the region $r \geq R_M$ outside of the sun. As we are not interested in the insides of the sun, we will work purely in that region from here onwards. To make that clear we will use the capital letter R for the distance from the sun, and $R_V^3 := 8\lambda^4 GM$ for the Vainshtein radius.

By putting the above solution back into Eq. (3.11) and then combining the resulting equation with Eq. (3.10) we get the modified Poisson equation

$$\nabla^2\Phi = 4\pi G a^2\mu^{NL}\bar{\rho}_m\delta, \tag{3.16}$$

where

$$\mu^{NL} := 1 + 2(\mu^L - 1)\left(\frac{R}{R_V}\right)^3\left[\sqrt{1 + \frac{R_V^3}{R^3}} - 1\right], \tag{3.17}$$

$$\mu^L := 1 + \frac{2\alpha_B^2}{\alpha c_s^2}. \tag{3.18}$$

By comparing the modified Poisson equation (3.16) with the ordinary Poisson equation (2.43), we see that μ^{NL} quantifies the effect of the modified gravity. Also notice that by linearising μ^{NL} around the overdensity δ we get μ^{L}. Hence the superscripts: L for linear and NL for non-linear.

The Galileon model reduces to GR in the limit $R \ll R_V$ where $\mu^{NL} = 1$. Therefore, we require from any Galileon theory that the Vainshtein radius R_V is much larger than the radius of our solar system. This mechanism is called Vainshtein screening. Furthermore, notice that the Vainshtein radius depends purely on α_B. Therefore, the Vainshtein screening arises from the term $G_3\Box\varphi$ in the Lagrangian. In fact, this screening arises even when $G_4 \neq 0$ as long as G_3 is present. We have shown the Vainshtein mechanism for a fairly simple system. But it is still present in more complicated systems [JJKT15, Kob19].

Other models of modified gravity can have different screening mechanisms. Vainshtein screening, for example, emerges form the second order derivative of φ becoming relatively large near massive objects, while kinetic screening emerges due to the first order derivatives becoming large. Other screening mechanisms depend on the effective mass of the additional field growing near regions of high density or on the coupling to matter becoming weak [JJKT15]. For our models, though, only the Vainshtein mechanism applies.

3.3 Spherical Collapse

While the Galileon models were introduced to explain dark energy, they also change other aspects of how the universe behaves, such as the formation of large scale structures. In Section 2.5 we have looked at the spherical collapse model of how dark matter halos form. Now, we want to change this model so as to accommodate the Galileon modified gravity theories. This would allow us to compare those models of modified gravity with the Λ-CDM model.

Notice that the assumptions used to derive the modified Poisson equation (3.16) are also used in the spherical collapse model. Furthermore, generalised cubic Galileon models only add scalar degrees of freedom and there is no anisotropic stress, therefore the equations (2.40) and (2.42) still hold.

By combining Eq. (2.42) with the modified Poisson equation (3.16) we

get the equation governing the radius of the overdense region:

$$\frac{\ddot{R}}{R} = H^2 + \dot{H} - \frac{4\pi G}{3} a^2 \mu^{NL} \overline{\rho}_m \delta. \tag{3.19}$$

To make numerical simulation of the above equation easier, we will perform a change of variables

$$y = \frac{R}{R_i} - \frac{a}{a_i}, \tag{3.20}$$

with R_i being the initial value of the radius of the perturbation and a_i being the initial value of the scale factor. This change of variables gives us the equation

$$y'' = -\frac{H'}{H} y' + \left(1 + \frac{H'}{H}\right) y - \frac{\Omega_m}{2} \mu^{NL} \delta \left(y + \frac{a}{a_i}\right), \tag{3.21}$$

with the primes representing a derivative with respect to $\ln a$ and Ω_m being the matter density parameter defined in Eq. (2.19). All functions of time will henceforth be reparametrised in terms of the scale factor a. This is possible because the scale factor increases monotonically with time. By setting $\mu^{NL} = 1$ we get the equation governing spherical collapse in the Λ-CDM model.

Using the conservation of mass (2.41) we can write the overdensity as

$$\delta = (1 + \delta_i) \left(1 + \frac{a_i}{a} y\right)^{-3} - 1, \tag{3.22}$$

where δ_i is the initial overdensity at a_i.

Notice that the mass used in the definition of Vainshtein radius is the mass of the overdensity alone, i.e. $4\pi\overline{\rho}_m\delta/3$. This gives us

$$\frac{R^3}{R_V^3} = \frac{1}{4\Omega_m H^2 \lambda^4} \frac{1}{\delta}. \tag{3.23}$$

Now, only the background parameters H, Ω_m, Ω_r and α_B are left unspecified in Equation (3.21). They will be treated separately in the following sections as they have to be calculated from the background equations.

To do the numerical simulations we need to know initial conditions. We will always take the initial scale factor to be $a_i = 10^{-5}$, which is well into the radiation dominated era. Then, it is obvious from the definition that $y_i = 0$. Furthermore, it follows from Equation (3.22) that $y_i' = -\frac{\delta_i'}{3(1+\delta)}$.

In Section 2.5, we saw that at first $\delta \propto a$, and thus $\delta' = \delta$. Since δ is a small perturbation we will assume that $(1+\delta) \approx 1$, which gives $y_i' = -\delta_i/3$. And finally δ_i will be chosen so that the collapse happens at some chosen time. Usually, we will choose for the collapse to happen right now, i.e. $a_{coll} = 1$.

However, remember that the spherical collapse model is needed to calculate the critical overdensity δ_c, which is then further used to get observable quantities. To determine it we need the linearised equation describing the evolution of δ. We already know the non-linear version of this equation Eq. (2.40). By combining it with the modified Poisson equation (3.16) and then linearising the result we get

$$\delta'' + \left(2 + \frac{H'}{H}\right)\delta' = \frac{3}{2}\Omega_m \mu^L \delta. \tag{3.24}$$

3.4 Background Equations

To be able to model the spherical collapse we still need to calculate the quantities H, Ω_m, Ω_r and α_B, which we can get by solving the background equations. Remember that the background is homogeneous and isotropic in space, as such all background parameters only depend on time. Since in the rest of this chapter we will only deal with the background parameters, we will write them without the overlines.

By putting the background parameters into the modified Einstein field equations (3.5) we get the following two equations, where the first equation comes from the 00-component and the second comes from the spatial components:

$$3M_{pl}^2 H^2 = \rho_m + \rho_r - 2G_{2X}\dot{\varphi}^2 - G_2 + 6HG_{3X}\dot{\varphi}^3, \tag{3.25}$$

$$M_{pl}^2(2\dot{H} + 3H^2) = 2G_{3X}\dot{\varphi}^2\ddot{\varphi} - G_2 - \frac{1}{3}\rho_r. \tag{3.26}$$

These two equations can be seen as the modified versions of the two Friedmann equations (2.13, 2.14). Then, from Eq(3.6) we get the equation of motion for the background scalar field φ:

$$\begin{aligned} 2G_{2XX}\dot{\varphi}^2\ddot{\varphi} - G_{2X}\ddot{\varphi} + 3\dot{H}G_{3X}\dot{\varphi}^2 - 6HG_{3XX}\ddot{\varphi}\dot{\varphi}^3 \\ +6HG_{3X}\dot{\varphi}^3\ddot{\varphi} - 3HG_{2X}\dot{\varphi} + 9H^2G_{3X}\dot{\varphi}^2 = 0. \end{aligned} \tag{3.27}$$

The background equations cannot be solved without specifying G_2 and G_3. Henceforth, we will use two models, which are called the Galileon

ghost condensate (GGC) and the covariant cubic Galileon (G3). GGC is given by

$$G_2 = a_1 X + a_2 X^2, \;\; G_3 = 3a_3 X, \tag{3.28}$$

and G3 is given by the same expressions, but with $a_2 = 0$.

In this model the modified Friedmann equation (3.25) becomes

$$3M_{pl}^2 H^2 = \rho_m + \rho_r - a_1\dot{\varphi}^2 + 3a_2\dot{\varphi}^4 + 18a_3 H\dot{\varphi}^3. \tag{3.29}$$

Just as in Section 2.3, we define the dimensionless parameters

$$x_1 := -\frac{a_1\dot{\varphi}^2}{3M_{pl}^2H^2}, \;\; x_2 := \frac{a_2\dot{\varphi}^4}{M_{pl}^2H^2}, \;\; x_3 := \frac{6a_3\dot{\varphi}^3}{M_{pl}^2H}, \tag{3.30}$$

so that the Friedmann equation can be rewritten into

$$\Omega_m + \Omega_r + \Omega_\varphi = 1, \tag{3.31}$$

where $\Omega_\varphi := x_1 + x_2 + x_3$ is the effective density parameter of the scalar field φ. Notice that to get the G3 model we just have to set $x_2 = 0$.

Using the Friedmann equation we can compute Ω_m from the other parameters. To find the dynamical system governing the other four parameters we will differentiate them with respect to $\ln a$ (denoted by prime). Remember from Section 2.3 that ρ_r scales as a^{-4}, which means that $\Omega_r \propto a^{-4}H^{-2}$. This gives the following system of differential equations:

$$x_1' = 2x_1(\varepsilon_\varphi - h), \tag{3.32}$$
$$x_2' = 2x_2(2\varepsilon_\varphi - h), \tag{3.33}$$
$$x_3' = x_3(3\varepsilon_\varphi - h), \tag{3.34}$$
$$\Omega_r' = -2\Omega_r(2 + h), \tag{3.35}$$

where $\varepsilon_\varphi := \ddot{\varphi}/(H\dot{\varphi})$ and $h := \dot{H}/H^2 = H'/H$. By solving the above equations we can get all the background parameters we need for spherical collapse. But first, we have to find the expressions for ε_φ and h in terms of the parameters above.

To do that we rewrite the second Friedmann equation (3.26) and the equation of motion (3.27) using the dimensionless parameters:

$$x_3\varepsilon_\varphi - 3x_1 - x_2 - \Omega_r - 3 - 2h = 0, \tag{3.36}$$
$$6x_1 + 4x_2 + 3x_3 + 2(x_1 + 2x_2 + x_3)\varepsilon_\phi + x_3 h = 0. \tag{3.37}$$

Then we combine these equation and get

$$\varepsilon_\varphi = -\frac{1}{q_s}[4(3x_1 + 2x_2) - x_3(3x_1 + x_2 + \Omega_r - 3)], \tag{3.38}$$

$$h = -\frac{1}{q_s}[2(3x_1 + x_2 + \Omega_r + 3)(x_1 + 2x_2) + 2x_3(6x_1 + 3x_2 + \Omega_r + 3) + 3x_3^2], \tag{3.39}$$

with

$$q_s := 4(x_1 + 2x_2 + x_3) + x_3^2. \tag{3.40}$$

Now, we have found all the equations necessary to simulate the evolution of the background. It only remains to connect the dimensionless parameters we used in this section with the quantities used in the previous section. The expressions for Ω_m and $H'/H = h$ have already been found. And the alpha parameters are given by

$$\alpha_B = -\frac{1}{2}x_2 \tag{3.41}$$

$$\alpha_K = 6(x_1 + 2x_2 + x_3) \tag{3.42}$$

$$\alpha = \frac{3}{2}q_s. \tag{3.43}$$

Then, using

$$\alpha_B' = -\frac{1}{2}x_3' = -\frac{1}{2}x_3(3\varepsilon_\varphi - h) \tag{3.44}$$

we can find the expressions for αc_s^2 and all the other necessary quantities.

There are also some other quantities which could be interesting to know. For example, the Hubble parameter can be calculated as follows

$$\frac{H^2}{H_0^2} = \frac{\Omega_{r0}}{a^4\Omega_r}, \tag{3.45}$$

where H_0 and Ω_{r0} are the current values of the Hubble parameter and the radiation density parameter.

From the modified Friedmann equations (3.25, 3.26) we can find the effective energy density ρ_φ and pressure p_φ of the scalar field. Using those we can find the effective equation of state parameter

$$w_\varphi := \frac{p_\varphi}{\rho_\varphi} = \frac{3x_1 + x_2 - x_3\varepsilon_\varphi}{3\Omega_\varphi}. \tag{3.46}$$

Version of July 4, 2024– Created July 4, 2024 - 22:11

As discussed in Section 2.3, this parameter determines how the scalar field affects the expansion of the universe. In particular, when $w_\varphi > -1/3$, then ϕ decelerates the expansion of the universe, while when $w_\varphi < -1/3$, then it accelerates the expansion.

3.5 Stability Analysis

For the dynamical system (3.32)-(3.35) to represent the physical world, it has to be well-behaved. A solution starting with physically meaningful initial conditions should remain physical. Furthermore, any solution with which we want to model our universe should approach the de Sitter universe, i.e. a universe that is dominated by dark energy with $w_{DE} = -1$. In this section we will show that there is a region of the phase space in which all solutions are indeed well-behaved.

First, we notice that the dynamical system is not defined on the region given by $q_s = 0$, but outside of that region it is continuously differentiable. By the Picard-Lindelöf theorem [Mei07, Th. 3.19] any initial condition $x_0 \in \mathbb{R}^4 \setminus \{q_s = 0\}$ at $a_0 \in \mathbb{R}$ has a unique solution $x(a)$ in some open interval around a_0 for which $x(a_0) = x_0$.

Then, it is trivial to see that any solution that starts at a hyperplane given by $x_1 = 0$, $x_2 = 0$, $x_3 = 0$ or $\Omega_r = 0$ must always stay on that hyperplane. It follows by uniqueness that all solutions must remain on the same side of those hyperplanes. So, all four components of a solution $x(a)$ must maintain their sign. This allows us to restrict our attention to the solutions with $x_1 < 0$, $x_2 \geq 0$, $x_3 > 0$ and $\Omega_r \geq 0$. Here the choice $x_2 > 0$ corresponds to the GGC model and the choice $x_2 = 0$ corresponds to the G3 model. The condition $\Omega_r \geq 0$ follows from it being the energy density parameter of radiation, as the energy of radiation cannot be negative. The reasons for the other choices will become clear later.

From the Friedmann equation (3.31) we can calculate that

$$\Omega_m' = -\Omega_m(3 + 2h). \tag{3.47}$$

This can also be seen from the definition 2.19 and from the fact the matter density ρ_m goes as a^{-3}. By similar reasoning as before we see that all solutions must stay on the same side of the hyperplane $\Omega_m = 0$. Just as for Ω_r we shall restrict our attention to the region where $\Omega_m \geq 0$.

There also exists another density parameter $\Omega_\varphi := x_1 + x_2 + x_3$, and, similarly to Ω_m and Ω_r, we want to restrict our attention to the region given by $\Omega_\varphi \geq 0$. But first, we have to check whether a solution that starts in that region stays in that region. To do that we will examine the

behaviour of the solutions near Ω_φ. In particular, we will look at $q_s\Omega'_\varphi$ with the substitution $x_1 = \Omega_\varphi - x_2 - x_3$. In that case we get

$$q_s\Omega'_\varphi = 8(x_2 + x_3)^2 + x_3^2 + \Omega_\varphi p(\Omega_\varphi, x_2, x_3), \tag{3.48}$$

where $p(\Omega_\varphi, x_2, x_3)$ is a polynomial. Then, we notice that $q_s = 4\Omega_\varphi + 4x_2 + x_3^2 > 0$ whenever $\Omega_\varphi \geq 0$, because $x_2 \geq 0$ and $x_3 > 0$. Therefore, $\Omega'_\varphi > 0$ on the hyperplane $\Omega_\varphi = 0$ where the system is defined. As such, no solution can cross this hyperplane from $\Omega_\varphi \geq 0$.

It follows that any solution that starts in the region $\Omega_\varphi \geq 0$ stays in that region. In addition, this implies that no solution in the given region approaches the hyperplane $\Omega_\varphi = 0$ as $a \to \infty$.

Notice that $q_s > \Omega_\varphi \geq 0$, therefore the aforementioned fact also shields our solutions from going towards $q_s = 0$. The solutions cannot even approach the region where $q_s = 0$.

However, the previous reasoning does not work when $\Omega_\varphi = q_s = 0$. So, in our region it does not work for the origin, which physically represents a universe without any dark energy or radiation and with unmodified gravity. But, sufficiently close to the origin we can assume that the second and higher order terms can be ignored in favour of the linear terms. Then, we get

$$q_s(\varepsilon_\varphi - h) \approx -6x_1 + 4x_2 + 3x_3 > 0. \tag{3.49}$$

In our region $q_s > 0$, therefore $\varepsilon_\varphi - h > 0$. Then by looking at Equation (3.32) we see that $x'_1 < 0$ near the origin. It follows that the x_1 component of any solution in our region must go away from the origin if the solution is close enough to the origin. Therefore, no solution in our region can approach or reach the origin. Notice that all three sign conditions for x_i have been used, so this can be seen as an explanation for those choices.

It is important to note that the previous statements only hold if we go forward in time. If, on the other hand, we go backwards in time then an almost reverse statement holds: any solution which is sufficiently close to the hyperplane Ω_φ shall cross it into the region where $\Omega_\varphi < 0$ and then most, if not all, solutions will cease to exist as they go into the region where $q_s = 0$. This will be important in Chapter 4, because through observations it is easier to get what those values are today than what they were in the early universe.

The Friedmann equation (3.31) then places the last restriction on our region with it being given by $0 \leq \Omega_m, \Omega_r, \Omega_\varphi \leq 1$. This restriction agrees with the physical interpretation of the energy density parameter as the

fraction of energy in some region which comes from its corresponding source.

We have now defined a region given by $x_1 < 0$, $x_2 \geq 0$, $x_3 > 0$ and $0 \leq \Omega_m, \Omega_r, \Omega_\varphi \leq 1$ and shown that any solution that starts in this region shall remain in it as long as we go forwards in time. This region is, however, unbounded. So now, we will look at the behaviour of the solutions which start far away from the origin.

Notice that for any point far away from the origin at least one of the parameters x_1, x_2 or x_3 must be large. Then, from $0 \leq \Omega_\varphi \leq 1$ we get $-x_2 - x_3 \leq x_1 \leq 1 - x_2 - x_3$. This, on its own part, implies that if any of the three parameters is large, then x_1 must also be large. Furthermore, it implies that $x_1 \approx -x_2 - x_3$. So, we have $x_1 \ll 0$ and $x_2 + x_3 \gg 0$. We will now assume that the parameters are sufficiently large so that linear terms and second order terms containing Ω_r can be ignored in favour of the second order terms of the form $x_i x_j$. Under these conditions we can show that $\varepsilon_\varphi - h, 2\varepsilon_\varphi - h, 3\varepsilon_\varphi - h < 0$. Then, the equations (3.32)-(3.34) imply that $x_1' > 0$ and $x_2', x_3' < 0$. Therefore, the solutions in our region cannot go to infinity as $a \to \infty$. Instead, all solution must have bounded forward orbits.

Now, we want to find which points the solutions can approach. To do that we will look at the fixed points within or at the border of our region. Notice that any fixed point must have $\Omega_r' = 0$. This condition is satisfied if $\Omega_r = 0$ or if $h = -2$. We shall first look at the case where $h = -2$. In this case precisely two of the three parameters x_i must be equal to zero, as otherwise either $q_s = 0$ or ε_φ must be equal to two different values at the same time.

The case where $x_2 = x_3 = 0$ leads to a contradiction and does not give any fixed points. The case where $x_1 = x_2 = 0$ and $x_3 \neq 0$ gives us the fixed point with $x_3 = -4$ and $\Omega_r = 3$. But, this fixed point is well outside our region of interest. So, we will ignore it. Lastly, the case where $x_1 = x_3 = 0$ gives us a line of fixed points $\Omega_r = 1 - x_2$. Physically, these solutions correspond to a universe without any matter. Furthermore, $w_\varphi = \frac{1}{3}$, so the scalar field acts just like radiation and those universes will at some point start to contract.

To compute the stability of the fixed points on this line we will use its Jacobian. The full expression for the Jacobian is given in appendix A.2,

while for these fixed points the Jacobian is given by

$$\begin{pmatrix} 2 & 0 & 0 & 0 \\ 3x_2 - 4 & x_2 & x_2 + 1 & x_2 \\ 0 & 0 & -1 & 0 \\ 3 - 3x_2 & 1 - x_2 & 1 - x_2 & 1 - x_2 \end{pmatrix}. \tag{3.50}$$

This matrix has eigenvalues -1, 0, 1 and 2 with the corresponding eigenvectors being $(0,0,1,0)$, $(0,1,0,-1)$, $(0,1,-1,0)$ and $(1,0,0,0)$.

By the centre manifold theorem [Mei07, Th. 5.21] we know that these fixed points must each have a 1-dimensional local centre manifold, a 1-dimensional local stable manifold and a 2-dimensional local unstable manifold with all being tangent to the respective eigenvectors. The centre manifold is just the line of fixed points $\Omega_r = 1 - x_2$. At the same time, if we reduce our system by setting $x_1 = 0$, then the stable manifold remains locally unchanged. Therefore, the stable manifold must be completely contained in the hyperplane given by $x_1 = 0$. It follows by the non-hyperbolic Hartman-Grobman theorem [Mei07, th. 5.21] that solutions in our region do not approach this set of fixed points as $a \to \infty$.

We have found all fixed points with the condition $h = -2$, now we continue to the fixed points with $\Omega_r = 0$. Once again, we start with the the cases where two of the x_i parameters are zero. First, the case where $x_1 = x_2 = 0$ gives us the fixed point with $x_3 = 1$. This fixed point physically corresponds to a universe without any matter or radiation. Furthermore, as $w_\varphi = \frac{3}{5}$, this universe shall eventually start to contract.

The Jacobian of this point is given by

$$\begin{pmatrix} \frac{12}{5} & 0 & 0 & 0 \\ 0 & \frac{6}{5} & 0 & 0 \\ -\frac{9}{5} & -\frac{3}{5} & \frac{3}{5} & 1 \\ 0 & 0 & 0 & -\frac{2}{5} \end{pmatrix}. \tag{3.51}$$

This matrix has eigenvalues $\frac{12}{5}$, $\frac{6}{5}$, $\frac{3}{5}$ and $-\frac{2}{5}$ with the corresponding eigenvectors being the standard basis vectors. By the stable manifold theorem [Mei07, Th. 5.9] we know that there is a 1-dimensional local stable manifold. The reduced dynamical system with $x_1 = 0$ still has a 1-dimensional local stable manifold for this fixed point. Therefore this stable manifold must be contained in the hyperplane $x_1 = 0$. This implies that no solutions starting in our given region will approach this fixed point as $a \to \infty$.

Now, we proceed with finding the fixed points. The case where $\Omega_r = x_1 = x_3 = 0$ gives us the fixed point given by $x_2 = 1$. But this point lies

on the line given by $\Omega_r = 1 - x_2$ and we have already looked at this set of fixed points.

The case where $\Omega_r = x_2 = x_3 = 0$, gives us the fixed point given by $x_1 = 1$. However, this point lies outside of the region at which we look. We will, therefore, ignore this fixed point.

Finally, we arrive at the last set of fixed points given by $\Omega_r = \varepsilon_\varphi = h = 0$. In this case we get a line of fixed points given by

$$x_3 = 1 - x_1 - x_2, \;\; x_2 = -3(x_1 + 1). \tag{3.52}$$

For these fixed points it holds that $\Omega_\varphi = 1$. They, therefore, represent a universe without any matter or radiation. Furthermore, $w_\varphi = -1$, so the scalar field acts like the cosmological constant in these universes. As such, these fixed points represent the de Sitter universe. Hence, those points are called the de Sitter fixed points. Notice that our region only contains the portion of this line for which $-2 \leq x_1 \leq -1$.

The Jacobian of these fixed points is given by

$$\frac{1}{q_s}\begin{pmatrix} 24x_1 & 4x_1x_3 & -4x_1x_2 & -8x_1^2 \\ 6x_2x_3 & 3x_2(3x_1+2) & 12x_1x_2 & -4x_2(x_1-2) \\ -4x_2x_3 & 8x_1x_2 & 6x_3(x_1-1) & 8x_3 \\ 0 & 0 & 0 & -4q_s \end{pmatrix}. \tag{3.53}$$

This matrix has eigenvalues 0, -4, -3 and -3. By the centre manifold theorem [Mei07, Th. 5.21] these fixed points have a 1-dimensional centre manifold which we know to be the line of the de Sitter fixed points. We can confirm this by noticing that the eigenvector $(1, -3, 2, 0)$ of the eigenvalue 0 gives the direction for the line of the de Sitter fixed points. Then, by the non-hyperbolic Hartman-Grobman theorem [Mei07, Th. 5.21] we know that there is some neighbourhood of the centre manifold so that the solutions which start in this open set approach the de Sitter fixed points. So, the collection of the de Sitter fixed points forms the de Sitter attractor.

We have now classified all the relevant fixed points and we found one attractor which the solutions in our region can approach. In addition, this attractor represents the de Sitter universe and we know that our universe is approaching that kind of state. Under the assumption that there are no other attractors within our region, we can say that all solutions starting there shall approach the de Sitter universe. And the numerical simulations indeed show that to be the case.

3.6 Tracker Solution

In the previous section we have shown for both the GGC and the G3 model that there exists an attractor which must be approached by all physically relevant solutions. However, in the G3 model we can make an even stronger statement: there exists a tracker solution which attracts other physically relevant solutions [DFT10] and which itself approaches the de Sitter fixed point. It has even been shown that any solution of the G3 model that does not approach the tracker solution fast enough has a poor fit to observational data [BLBP14].

This tracker solution is given by the condition that $H\dot{\varphi}$ is constant. By differentiating this condition we get the equation $\varepsilon_\varphi = -h$. From it we get the following condition

$$x_3 = -2x_1. \tag{3.54}$$

Using this we can rewrite Eq. (3.46) to get the following expression for the equation of state parameter:

$$w_{DE} = -1 + \frac{2}{3}h. \tag{3.55}$$

In a matter-dominated universe the terms corresponding to the radiation and the scalar field can be neglected when compared to the matter terms. In that regime the Friedmann equations (3.25) and (3.26) give us $h \approx -\frac{3}{2}$. So, in a universe following the tracker the scalar field φ has $w_{DE} \approx -2$ during matter dominance. But this contradicts the observations of our universe [NDFT10]. So, the G3 model is unlikely to represent our universe.

But it can still serve well to compare with the GGC models. In particular, because the tracker has an analytic solution for the Hubble parameter given by

$$\frac{H}{H_0} = \sqrt{\frac{1}{2}\left(\Omega_{r0}a^{-4} + \Omega_{m0}a^{-3} + \sqrt{(\Omega_{r0}a^{-4} + \Omega_{m0}a^{-3})^2 + 4\Omega_{\varphi 0}}\right)}, \tag{3.56}$$

where H_0, Ω_{m0}, Ω_{r0} and $\Omega_{\varphi 0}$ represent the current values of the Hubble parameter and the matter, radiation and scalar field energy density parameters respectively. Then, if we use that $H\dot{\varphi}$ is constant and that radiation density $\rho_r \propto a^{-4}$, we can write the two remaining free terms of the system as

$$x_1 = -\Omega_{\varphi 0}\frac{H_0^4}{H^4}, \quad \Omega_r = \frac{\Omega_{r0}}{a^4}\frac{H_0^2}{H^2}. \tag{3.57}$$

Version of July 4, 2024– Created July 4, 2024 - 22:11

Notice that Ω_{m0} can be determined as follows $\Omega_{m0} = 1 - \Omega_{r0} - \Omega_{\varphi 0}$. Therefore, in the G3 model with the tracker solution, the background evolution can be solved analytically and it is completely determined by Ω_{r0} and $\Omega_{\varphi 0}$. This gives us all the required information to simulate spherical collapse with Eq. (3.21).

The best fit value for Ω_{m0} in this model was found to be 0.266 ± 0.004 [PFH$^+$18]. We will, for simplicity, round that number to $\Omega_{m0} = 0.27$. For Ω_{r0} we will take the Λ-CDM value $8.516 \cdot 10^{-5}$ as given in Section 2.3. This gives $\Omega_{\varphi 0} = 0.73$. With these values we calculate the evolution of the density and the equation of state parameters. It is given in Fig. 3.1. In the figure we can see that the evolution of the density parameters happens roughly in the same way as in the Λ-CDM model (Fig. 2.1). The equation of state parameter indeed goes to $w_\varphi = -2$, while during the radiation dominated era it is even lower. When approaching the dark energy dominated era w_φ goes to -1, thereby replicating the behaviour of the cosmological constant Λ.

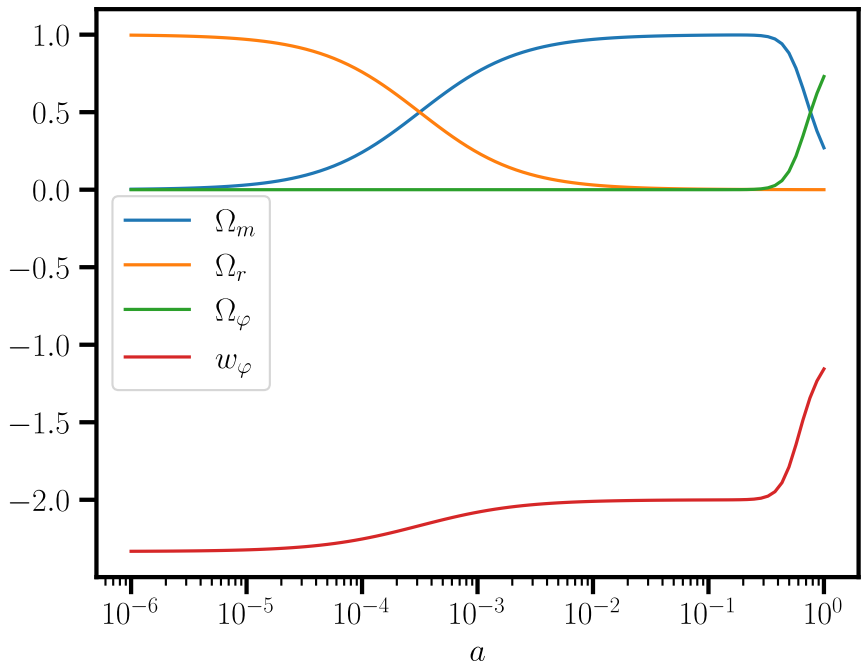

Figure 3.1: *Evolution of the density parameters Ω_i and the equation of state parameter w_φ in the G3 model with the tracker solution as a function of the scale factor. The current values of the density parameters are set to $\Omega_{\varphi 0} = 0.73$, $\Omega_{m0} = 0.27$ and $\Omega_{r0} = 8.516 \cdot 10^{-5}$.*

Chapter 4

Simulations

First, we will numerically solve the background equations for different initial values. We will also characterise what initial values give solutions that exist far enough into the past. Then, the spherical collapse will be modelled for several of the initial values. In addition, we will look at how changes in initial parameters affect the critical overdensity.

All initial value problems in this chapter are solved using the Runge-Kutta method of order 5(4) as it is implemented in *scipy.integrate.solve_ivp*.

4.1 Background

To simulate the evolution of the background in the GGC model we need to find appropriate initial conditions. For the current radiation density parameter value we will continue to use the Λ-CDM value $\Omega_{r0} = 8.516 \cdot 10^{-5}$. In [PBFT19] the GGC model was fit to two different datasets which they called Planck and PBRS. Planck gave $x_1^{(0)} = -1.26 \pm 0.2$, $x_2^{(0)} = 1.64 \pm 0.5$ and $x_3^{(0)} = 0.34 \pm 0.4$ as the maximum likelihood values, while PBRS gave $x_1^{(0)} = -1.27 \pm 0.1$, $x_2^{(0)} = 1.74 \pm 0.2$ and $x_3^{(0)} = 0.23 \pm 0.1$. Here $x_i^{(0)}$ refers to the current value of the corresponding parameter x_i with $i = 1, 2, 3$.

The dynamical system (3.32)-(3.35) can then be solved backwards in time with the above initial conditions. The resulting background evolution can be seen in Fig. 4.1. Remember that the scale factor a is normalised, so that its current values is $a = 1$. The figure shows that the evolution does not differ qualitatively between the Planck and PBRS initial conditions.

However, both simulations show an additional period between the

matter and radiation dominated eras where the scalar field dominates. This period is not seen in either the G3 (Fig. 3.1) or the Λ-CDM (Fig. 2.1) models. Though, notice that the equation of state parameter w_φ of the scalar field is between the equation of state parameters of matter $w_m = 0$ and of radiation $w_r = \frac{1}{3}$. So, this should not have a significant effect on the expansion of the universe.

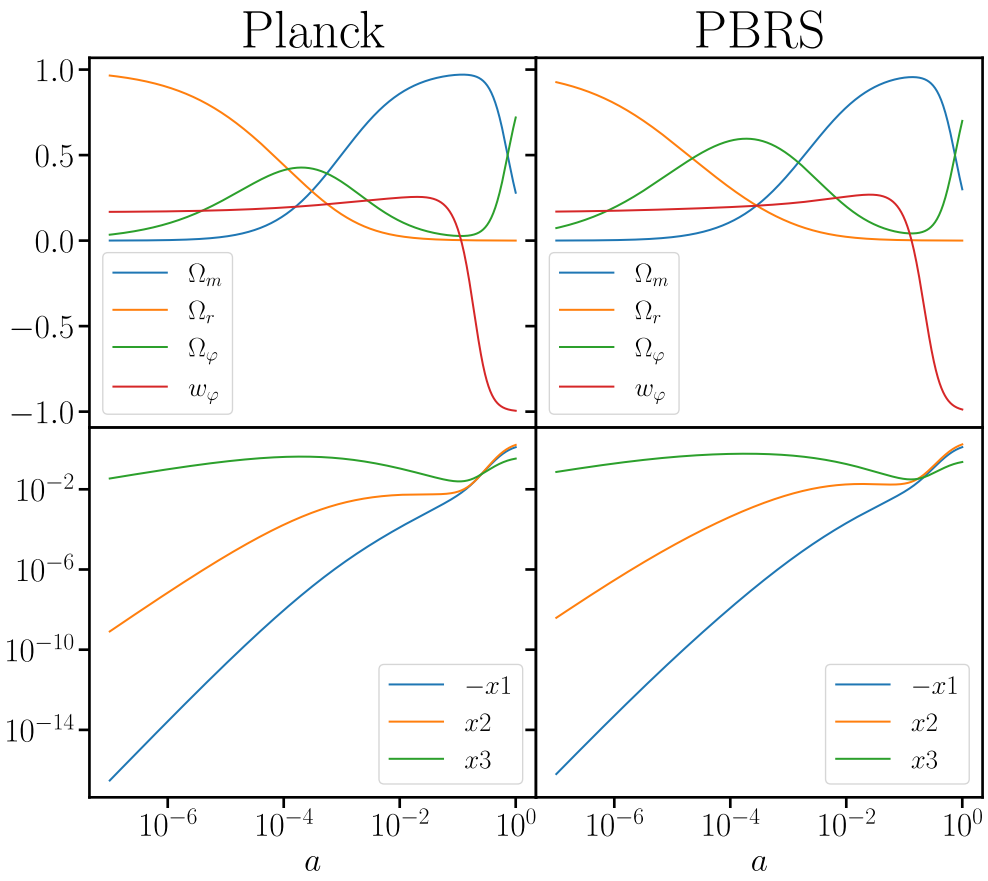

Figure 4.1: *Evolution of Ω_m, Ω_r, Ω_φ, w_φ (top) and $-x_1$, x_2 and x_3 (bottom) in the GGC model as a function of the scale factor. The initial conditions are given by $x_1^{(0)} = -1.26$, $x_2^{(0)} = 1.64$, $x_3^{(0)} = 0.34$, $\Omega_{r0} = 8.516 \cdot 10^{-5}$ (left) and by $x_1^{(0)} = -1.27$, $x_2^{(0)} = 1.74$, $x_3^{(0)} = 0.23$, $\Omega_{r0} = 8.516 \cdot 10^{-5}$ (right) at the present era $a = 1$. The simulation is performed backwards in time.*

It might, however, have an effect on the spherical collapse, since Eq. (3.21) has an explicit dependence on Ω_m, which does change due to the intermediary era dominated by the scalar field. As such, we would like to get some GGC models where there is no additional period of scalar field domination. This can be achieved by reducing $x_3^{(0)}$ to 0.334 for the Planck

values and to 0.221 for the PBRS values. We will call the models with these values Modified Planck and Modified PBRS or MPlanck and MPBRS for short. The resulting evolution can be see in Fig. 4.2.

The resulting evolution of x_1, x_2 and x_3 does not differ significantly in form from the unmodified Planck and PBRS cases. However, the absolute values of these parameters is roughly an order of magnitude smaller. This leads to the absence of the additional period where the scalar field dominates.

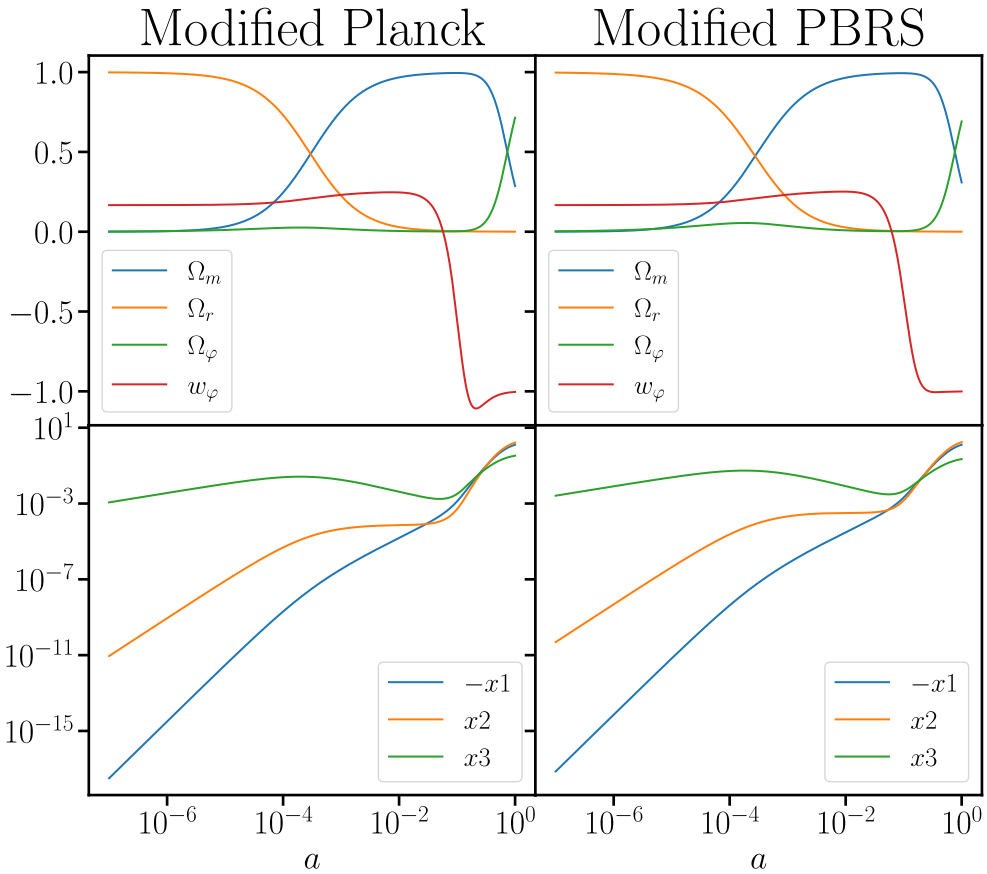

Figure 4.2: *Evolution of Ω_m, Ω_r, Ω_φ, w_φ (top) and $-x_1$, x_2 and x_3 (bottom) in the GGC model as a function of the scale factor. The initial conditions are given by $x_1^{(0)} = -1.26$, $x_2^{(0)} = 1.64$, $x_3^{(0)} = 0.334$, $\Omega_{r0} = 8.516 \cdot 10^{-5}$ (left) and by $x_1^{(0)} = -1.27$, $x_2^{(0)} = 1.74$, $x_3^{(0)} = 0.221$, $\Omega_{r0} = 8.516 \cdot 10^{-5}$ (right) at the present era $a = 1$. The simulation is performed backwards in time.*

A follow-up question is what happens when we decrease $x_3^{(0)}$ even further. If we set $x_3^{(0)}$ to 0.22 in PBRS, then the system will reach the singularity $q_s = 0$ at $a \approx 10^{-3}$, while if we set $x_3^{(0)}$ to 0.333 in Planck, then the

Version of July 4, 2024– Created July 4, 2024 - 22:11

system will reach the singularity even faster at $a \approx 10^{-1}$. Notice that this is well within the 95% confidence intervals given in [PBFT19].

We now want to see for which initial values the system will and for which it won't reach the singularity $q_s = 0$. To do that we will hold $\Omega_{m0} = 1 - x_1^{(0)} - x_2^{(0)} - x_3^{(0)} - \Omega_{r0}$ and Ω_{r0} constant and then we will vary $x_2^{(0)}$ and $x_3^{(0)}$, while calculating $x_1^{(0)}$ from the other parameters so that the Friedmann equation (3.31) is satisfied. We will do that for $\Omega_{m0} = 0.28, 0.30, 0.32$. The result can be seen in Fig. 4.3. In that figure a small blue dot was placed at the initial conditions for which the solution exists at least up until $a = 10^{-7}$. This region will be called non-singular region, while the other region where the solutions reach $q_s = 0$ will be called singular.

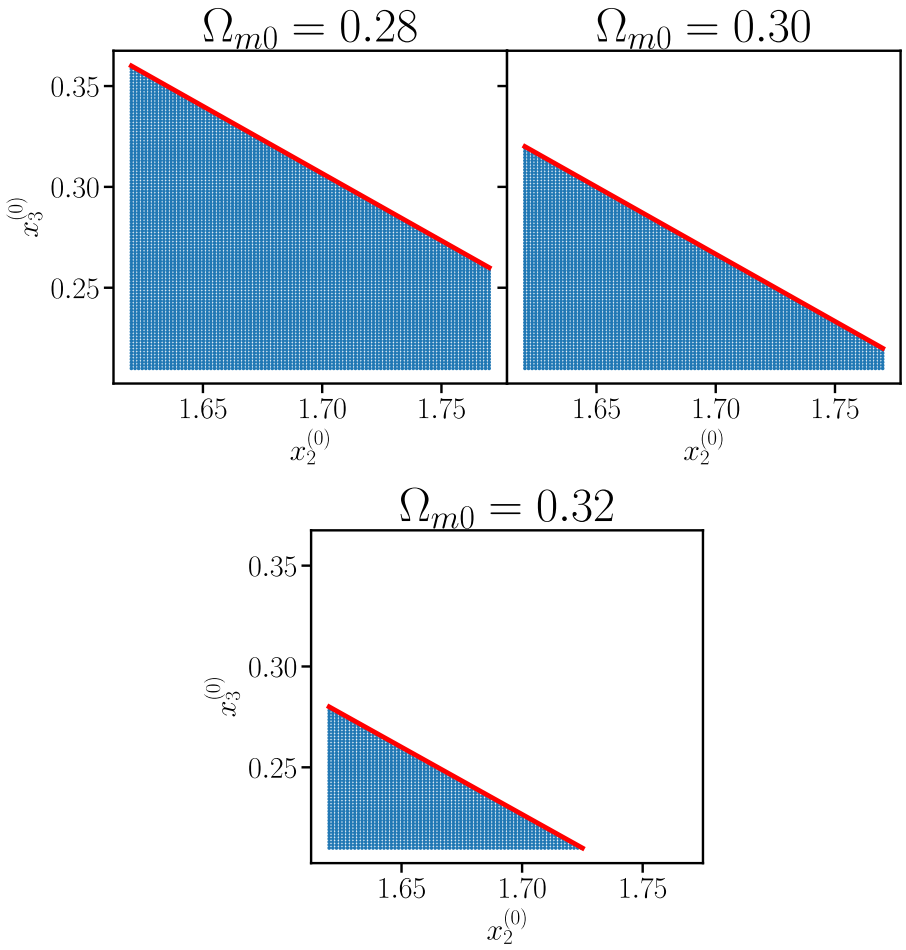

Figure 4.3: *The values of $x_2^{(0)}$ and $x_3^{(0)}$ at $\Omega_{m0} = 0.28, 0.30, 0.32$ and $\Omega_{r0} = 8.516 \cdot 10^{-5}$, so that the solutions starting at those values do not reach the singularity $q_s = 0$ and exist up until $a = 10^{-7}$. The red lines are given by $2x_2^{(0)} + 3x_3^{(0)} + 6\Omega_{m0} = 6$ and represent the boundaries between the singular and non-singular regions.*

In Fig. 4.3, there is also a red line in each of the graphs. This line is given by the equation $2x_2^{(0)} + 3x_3^{(0)} + 6\Omega_{m0} = 6$. As can be seen, it describes the boundary between the singular and non-singular region extremely well. In fact we have also fit the boundary of each graph to a line and we got $x_3^{(0)} = (1.439 \pm 0.002) - (0.666 \pm 0.001) \cdot x_2^{(0)}$ at $\Omega_{m0} = 0.28$, $x_3^{(0)} = (1.398 \pm 0.002) - (0.6666 \pm 0.0009) \cdot x_2^{(0)}$ at $\Omega_{m0} = 0.30$ and $x_3^{(0)} = (1.359 \pm 0.003) - (0.666 \pm 0.001) \cdot x_2^{(0)}$ at $\Omega_{m0} = 0.32$. The equation for the red lines is well within the bounds given by the fit.

If we neglect Ω_{r0} as it is small compared to the other values, we can rewrite the equation for the red lines to $6x_1^{(0)} + 2x_2^{(0)} + 3x_3^{(0)} = 0$. We will now define the quantity $d_0 := 6x_1^{(0)} + 2x_2^{(0)} + 3x_3^{(0)}$. From Fig. 4.3 it seems as if the solutions reach the singularity whenever $d_0 < 0$, while they continue to exist if $d_0 > 0$. Note that $d_0 = 0.02$, $d_0 = 0.03$, $d_0 = 0.002$, $d_0 = 0.001$ for Planck, PBRS, Modified Planck and Modified PBRS respectively. This suggests us to look at what happens when d_0 is small.

The evolution in Fig. 4.4 is given by the same initial parameters as PBRS but with $x_3^{(0)} = 0.22 + 2 \cdot 10^{-15}$; this gives $d_0 = 6 \cdot 10^{-15}$. So, we see that we can come really close to the surface $d_0 = 0$, while still having a non-singular solution. Though, it is difficult to see how small exactly we can make d_0 due to numerical errors. For example, if we use the standard settings of *scipy.integrate.solve_ivp*, then the solution as above but with varying $x_3^{(0)}$ will reach the singularity already at $x_3^{(0)} = 0.22 + 1.5 \cdot 10^{-15}$. However, if we increase the tolerances to the maximum value allowed, then the singularity won't be reached until around $x_3^{(0)} = 0.22 + 0.5 \cdot 10^{-15}$.

The behaviour of the solutions with small d_0 is similar to what we see in Fig. 4.4. In them the x_2 term quickly becomes much smaller than the x_1 and x_2. As a result, the solutions behave similarly to the G3 tracker solution with $w_\varphi \approx -2$ during the matter dominated era. However, they separate from the tracker solution at the transition between the matter and radiation dominated eras. This comes as a result of the x_1 term becoming much smaller than x_3 during that era.

Now, we will examine what happens when d_0 becomes relatively large. Figure 4.4 is made using once again the same initial parameters as PBRS but now with $x_3^{(0)} = 0.32$; this gives $d_0 = 0.3$. Here, we see the same scalar field dominated era between the matter and radiation dominated eras as in Fig. 4.1, however this era is much more prominent and takes up more time here than in Planck and PBRS.

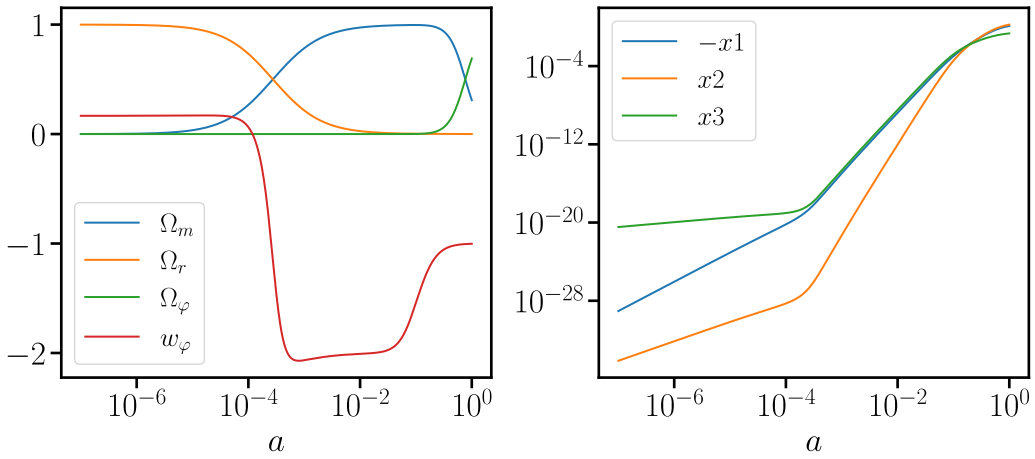

Figure 4.4: *Evolution of Ω_m, Ω_r, Ω_φ, w_φ (left) and $-x_1$, x_2 and x_3 (right) in the GGC model as a function of the scale factor. The initial conditions are given by $x_1^{(0)} = -1.27$, $x_2^{(0)} = 1.74$, $x_3^{(0)} = 0.22 + 2 \cdot 10^{-15}$, $\Omega_{r0} = 8.516 \cdot 10^{-5}$ at the present era $a = 1$. The simulation is performed backwards in time.*

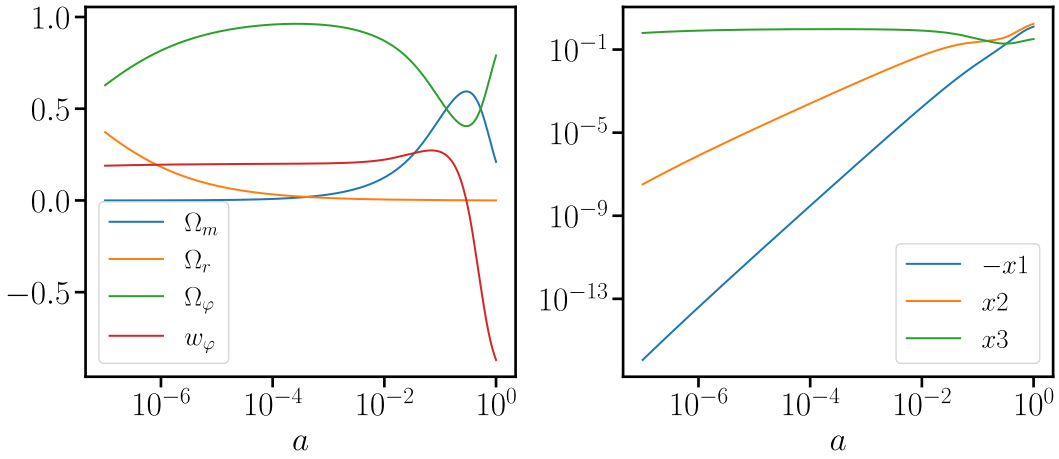

Figure 4.5: *Evolution of Ω_m, Ω_r, Ω_φ, w_φ (left) and $-x_1$, x_2 and x_3 (right) in the GGC model as a function of the scale factor. The initial conditions are given by $x_1^{(0)} = -1.27$, $x_2^{(0)} = 1.74$, $x_3^{(0)} = 0.32$, $\Omega_{r0} = 8.516 \cdot 10^{-5}$ at the present era $a = 1$. The simulation is performed backwards in time.*

4.2 Collapse

In Section 3.3 we have seen that the initial conditions of the dynamical system (3.21) are given by $a_i = 10^{-5}$, $y_i = 0$, $y_i' = -\delta_i/3$ and δ_i is chosen so that the collapse happens at some chosen time a_{coll}. We will calculate δ_i

using *scipy.integrate.solve_bvp*. This function requires a test solution which will then be relaxed into the desired solution. As the test solution we will use the analytical expression for spherical collapse given in Section 2.5.

First, we will solve spherical collapse for the GGC model with the Planck, Modified Planck, PBRS and Modified PBRS initial conditions for the background. Those solutions will be compared with the Λ-CDM and G3 tracker solutions. For the background of Λ-CDM and G3 tracker we will take the same values as in Fig. 2.1 and Fig. 3.1 respectively.

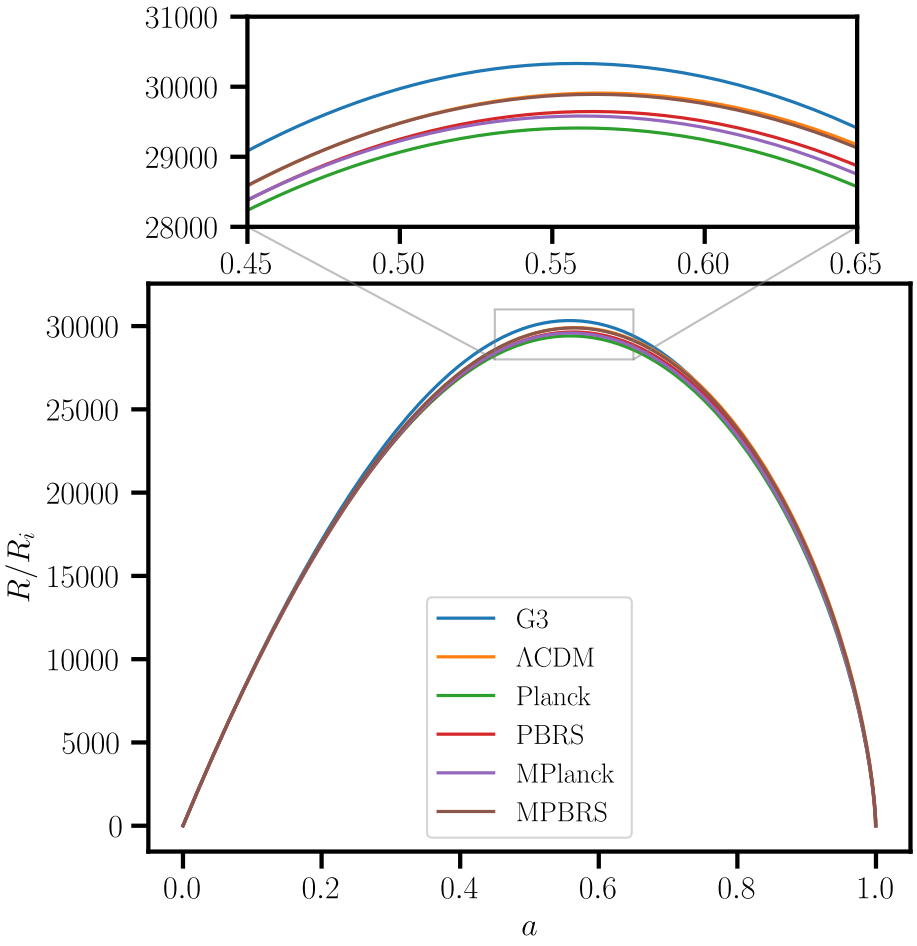

Figure 4.6: *Evolution of the radius of the spherical overdensity for different models. The initial conditions are chosen so that $a_{coll} = 1$. The initial overdensities are given by $\delta_i = 1.36 \cdot 10^{-4}$, $\delta_i = 1.44 \cdot 10^{-4}$, $\delta_i = 3.34 \cdot 10^{-4}$, $\delta_i = 5.23 \cdot 10^{-4}$, $\delta_i = 1.53 \cdot 10^{-4}$ and $\delta_i = 1.49 \cdot 10^{-4}$ for Λ-CDM, G3 with tracker, Planck, PBRS, Modified Planck, Modified PBRS*

If we choose the collapse to happen during the present era $a_{coll} = 1$, then we get Fig. 4.6. It shows how the radius of the spherical overdensity

changes with time. In it we see that the spherical overdensities behave similarly in all models. Their trajectories only slightly differ when the overdensities have reached their maximal extent.

Now, we will look at the critical overdensities of the aforementioned models. Figure 4.7 shows how the critical overdensity changes if we vary the collapse time. We notice that in all models except for G3 either the critical overdensity starts to decrease as a_{coll} increases or it is almost starting to decrease. Another pattern we notice is that Planck and PBRS models have a much steeper slope at early a_{coll}. Notice that this happens at a critical point of $\Omega_{\varphi 0}$. Therefore, this could come due to the intermediary scalar field dominated era in those models.

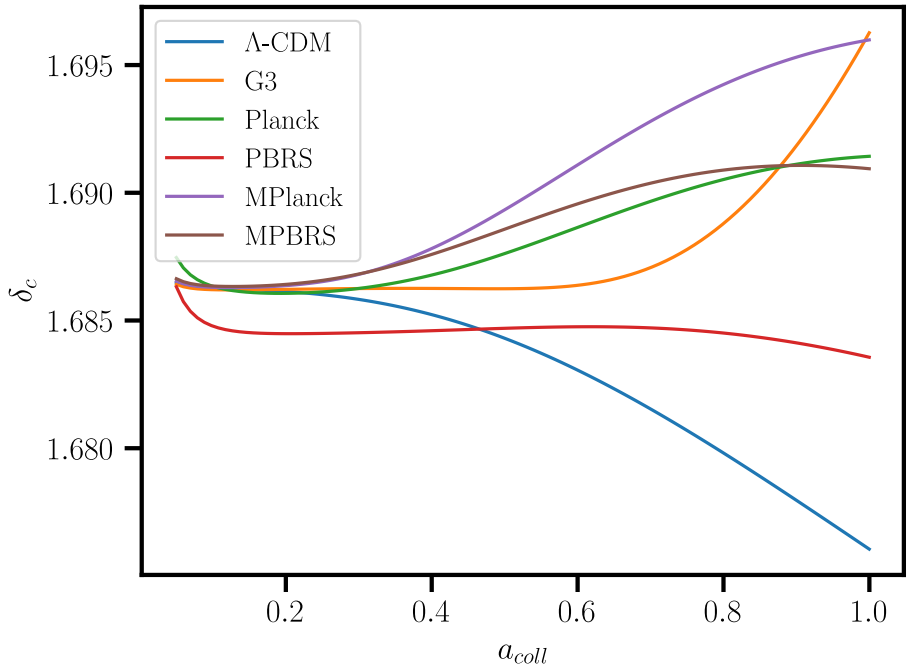

Figure 4.7: *Evolution of critical overdensity δ_c as a function of collapse time a_{coll} for the Λ-CDM model, the G3 model with tracker and the 4 GGC models.*

Lastly, we will look at the critical density changes if we change the initial conditions for the background evolution in the GGC models. As it is difficult to vary the terms x_1, x_2 and x_3 on their own, we will instead vary d_0, Ω_{m0} and $x_1^{(0)}$. We will take the initial values of the Planck, PBRS, MPlanck and MPBRS and then vary one of the three parameters while holding the other parameters still. Notice, however, that here we assume that the only difference between Planck and MPlanck, and PBRS and MPBRS is their d_0 value. This gives us Fig. 4.8.

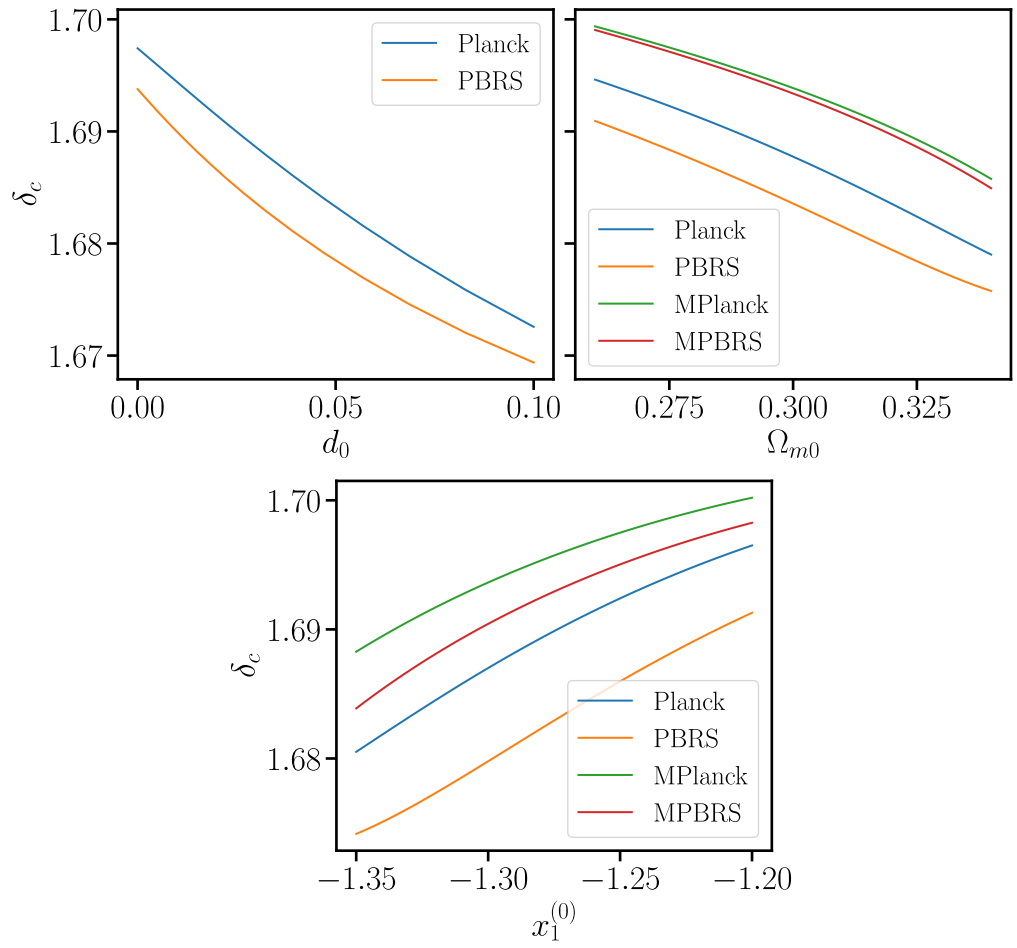

Figure 4.8: *Evolution of the critical overdensity δ_c as a function of the reparametrised initial conditions d_0, Ω_{m0} and $x_1^{(0)}$ for the background evolution.*

Chapter 5

Discussion

In Section 3.5 we have shown that a solution that starts in a certain reasonable region cannot reach the region $q_s = 0$, where the dynamical system for the background becomes singular, as long as we go forwards in time. However, in Chapter 4 we had to solve that equation backwards in time. While doing that, we found that there is a fairly clear boundary between the solutions which reach $q_s = 0$ and those that do not. This boundary is given by $d_0 = 0$.

Furthermore, the solutions seem to have a clear behaviour as they go away from the boundary. Close to $d_0 = 0$, there is no scalar field dominated era between the matter and radiation dominated eras. However, $w_\varphi = -2$ during the matter dominated era. Then, as d_0 increases, w_φ shall increase in the matter dominated era. Around $d_0 \approx 10^{-3}$, w_φ rises to roughly 0.3 during the matter dominated era. But at the same time, the intermediary scalar field dominated era appears. As d_0 increases further, the intermediary era becomes more prominent. As such it seems that the physical solutions appear in a fairly narrow band of d_0.

In further research, the backwards asymptotics of the background dynamical system could be studied more. In particular the exact shape of the boundary between the singular and non-singular regions. This could also allow to better specify the values of x_1, x_2 and x_3 in the present era together with their confidence interval. As, for example, in [PBFT19] the 95% confidence interval contains both trajectories which reach $q_s = 0$ and trajectories without a clear matter dominated era.

Then, we saw that different models can give fairly diverging values of critical overdensity in the spherical collapse model. Furthermore, even only within the GGC model different initial conditions can give rise to different critical overdensities. At the same time, each of d_0, Ω_{m0} and $x_1^{(0)}$

seems to influence δ_c fairly consistently and monotonically.

Further research could conduct a more systematic search through the different possible initial conditions of the GGC model to see how they influence the value of the critical overdensity. Furthermore, the critical overdensities could be converted into observable quantities, which then could be used in further research to constrain the possible initial conditions of the GGC model.

Version of July 4, 2024– Created July 4, 2024 - 22:11

Appendix A

Miscellaneous Expressions

A.1 Christoffel Symbols

The perturbed FLRW metric in the Newtonian Gauge is

$$ds^2 = -(1+2\Psi)dt^2 + a^2(t)(1-2\Phi)\delta_{ij}dx^i dx^j. \tag{A.1}$$

In this gauge the linearised Christoffel symbols are given by

$$\begin{aligned}
\Gamma^0_{0\mu} &= \partial_\mu \Psi & \Gamma^0_{ij} &= a^2\delta_{ij}(H - \dot{\Phi} - 2H(\Psi+\Phi)) \\
\Gamma^i_{00} &= a^{-2}\delta^{ij}\partial_j\Phi & \Gamma^j_{ji} &= -\partial_i\Phi \\
\Gamma^i_{j0} &= (H-\dot{\Phi})\delta^i_j & \Gamma^i_{jk} &= \Gamma'^i_{jk} - 2\delta^i_{(j}\partial_{k)}\Phi + \delta_{jk}\delta^{il}\partial_l\Phi,
\end{aligned} \tag{A.2}$$

where Γ'^i_{jk} are the Christoffel symbols of the Euclidean metric δ_{ij}. The linearised Ricci tensor components and the Ricci scalar are

$$\begin{aligned}
R_{00} &= \frac{\nabla^2\Psi}{a^2} - 3\dot{H} + 3\ddot{\Phi} + 3H\dot{\Psi} + 6H\dot{\Phi} - 3H^2 \\
R_{i0} &= 3H\partial_i(\Psi - \Phi) \\
R_{ij} &= a^2\delta_{ij}\left[3H^2 + \dot{H} - \ddot{\Phi} - 6H\dot{\Phi} - H\dot{\Psi} - 2(\dot{H}+3H^2)(\Psi+\Phi) + 2\frac{\nabla^2\Phi}{a^2} - \frac{\nabla^2\Psi}{a^2}\right] \\
R &= 6(\dot{H}+2H^2) - 6\ddot{\Phi} - 6H(\dot{\Psi}+4\dot{\Phi}) - 12(\dot{H}+2H^2)\Psi + 6\frac{\nabla^2\Phi}{a^2} - 4\frac{\nabla^2\Psi}{a^2}.
\end{aligned} \tag{A.3}$$

And the 00-component of the Einstein tensor is given by

$$G_{00} = 3H^2 + 6H\dot{\Phi} + 3\frac{\nabla^2\Phi}{a^2} - \frac{\nabla^2\Psi}{a^2}. \tag{A.4}$$

A.2 Jacobian

The Jacobian of the dynamical system (3.32)-(3.35) has the following components:

$$\frac{\partial x_1'}{\partial x_1} = 2\varepsilon_\varphi - 2h + \frac{2x_1}{q_s}\left(12x_1 + 14x_2 + 15x_3 + 2\Omega_r - 4\varepsilon_\varphi + 4h - 6\right),$$
$$\frac{\partial x_1'}{\partial x_2} = \frac{2x_1}{q_s}\left(14x_1 + 8x_2 + 7x_3 + 4\Omega_r - 8\varepsilon_\varphi + 8h + 4\right),$$
$$\frac{\partial x_1'}{\partial x_3} = \frac{2x_1}{q_s}\left(15x_1 + 7x_2 + 6x_3 + 3\Omega_r - 4\varepsilon_\varphi + 4h - 2x_3\varepsilon_\varphi + 2x_3h + 3\right),$$
$$\frac{\partial x_1'}{\partial \Omega_r} = \frac{2x_1}{q_s}\left(2x_1 + 4x_2 + 3x_3\right),$$
$$\frac{\partial x_2'}{\partial x_1} = \frac{2x_2}{q_s}\left(12x_1 + 14x_2 + 18x_3 + 2\Omega_r - 8\varepsilon_\varphi + 4h - 18\right),$$
$$\frac{\partial x_2'}{\partial x_2} = 4\varepsilon_\varphi - 2h + \frac{2x_2}{q_s}\left(14x_1 + 8x_2 + 8x_3 + 4\Omega_r - 16\varepsilon_\varphi + 8h - 4\right),$$
$$\frac{\partial x_2'}{\partial x_3} = \frac{2x_2}{q_s}\left(18x_1 + 8x_2 + 6x_3 + 4\Omega_r - 8\varepsilon_\varphi + 4h - 4x_3\varepsilon_\varphi + 2x_3h\right),$$
$$\frac{\partial x_2'}{\partial \Omega_r} = \frac{2x_2}{q_s}\left(2x_1 + 4x_2 + 4x_3\right),$$
$$\frac{\partial x_3'}{\partial x_1} = \frac{x_3}{q_s}\left(12x_1 + 14x_2 + 21x_3 + 2\Omega_r - 12\varepsilon_\varphi + 4h - 30\right),$$
$$\frac{\partial x_3'}{\partial x_2} = \frac{x_3}{q_s}\left(14x_1 + 8x_2 + 9x_3 + 4\Omega_r - 24\varepsilon_\varphi + 8h - 12\right),$$
$$\frac{\partial x_3'}{\partial x_3} = 3\varepsilon_\varphi - h + \frac{x_3}{q_s}\left(21x_1 + 9x_2 + 6x_3 + 5\Omega_r - 12\varepsilon_\varphi + 4h - 6x_3\varepsilon_\varphi + 2x_3h - 3\right),$$
$$\frac{\partial x_3'}{\partial \Omega_r} = \frac{x_3}{q_s}\left(2x_1 + 4x_2 + 5x_3\right),$$
$$\frac{\partial \Omega_r'}{\partial x_1} = \frac{2\Omega_r}{q_s}\left(12x_1 + 14x_2 + 12x_3 + 2\Omega_r + 4h + 6\right),$$
$$\frac{\partial \Omega_r'}{\partial x_2} = \frac{2\Omega_r}{q_s}\left(14x_1 + 8x_2 + 6x_3 + 4\Omega_r + 8h + 12\right),$$
$$\frac{\partial \Omega_r'}{\partial x_3} = \frac{2\Omega_r}{q_s}\left(12x_1 + 6x_2 + 6x_3 + 2\Omega_r + 4h + 2x_3h + 6\right),$$
$$\frac{\partial \Omega_r'}{\partial \Omega_r} = -4 - 2h + \frac{2\Omega_r}{q_s}(2x_1 + 4x_2 + 2x_3).$$

Version of July 4, 2024– Created July 4, 2024 - 22:11

Bibliography

[AAA+20] N. Aghanim, Y. Akrami, M. Ashdown, J. Aumont, C. Baccigalupi, M. Ballardini, A. J. Banday, R. B. Barreiro, N. Bartolo, S. Basak, R. Battye, K. Benabed, J.-P. Bernard, M. Bersanelli, P. Bielewicz, J. J. Bock, J. R. Bond, J. Borrill, . . . , A. Zacchei, and A. Zonca. Planck2018 results: Vi. cosmological parameters. *Astronomy & Astrophysics*, 641:A6, September 2020.

[AFPS24] Inês S. Albuquerque, Noemi Frusciante, Francesco Pace, and Carlo Schimd. Spherical collapse and halo abundance in shift-symmetric galileon theory. *Phys. Rev. D*, 109:023535, Jan 2024.

[Bau22] Daniel Baumann. *Cosmology*. Cambridge University Press, 2022.

[Bel12] Ari Belenkiy. Alexander Friedmann and the origins of modern cosmology. *Physics Today*, 65(10):38–43, 2012.

[BLBP14] Alexandre Barreira, Baojiu Li, Carlton M. Baugh, and Silvia Pascoli. The observational status of galileon gravity after planck. *Journal of Cosmology and Astroparticle Physics*, 2014(08):059–059, August 2014.

[BS14] Emilio Bellini and Ignacy Sawicki. Maximal freedom at minimum cost: linear large-scale structure in general modifications of gravity. *Journal of Cosmology and Astroparticle Physics*, 2014(07):050, jul 2014.

[Car19] Sean M Carroll. *Spacetime and geometry: An introduction to general relativity*. Cambridge University Press, 2019.

[DFT10] Antonio De Felice and Shinji Tsujikawa. Cosmology of a covariant galileon field. *Physical Review Letters*, 105(11), September 2010.

[Gam56] George Gamow. The evolutionary universe. *Scientific American*, 195(3):136–156, 1956.

[Hor74] Gregory Walter Horndeski. Second-order scalar-tensor field equations in a four-dimensional space. *International Journal of Theoretical Physics*, 10(6):363–384, Sep 1974.

[HS24] Gregory W. Horndeski and Alessandra Silvestri. 50 years of Horndeski gravity: Past, present and future. *International Journal of Theoretical Physics*, 63(2), February 2024.

[JJKT15] Austin Joyce, Bhuvnesh Jain, Justin Khoury, and Mark Trodden. Beyond the cosmological standard model. *Physics Reports*, 568:1–98, March 2015.

[Kob19] Tsutomu Kobayashi. Horndeski theory and beyond: a review. *Reports on Progress in Physics*, 82(8):086901, July 2019.

[Lee18] John M Lee. *Introduction to Riemannian manifolds*. Springer, 2 edition, 2018.

[LVFI17] LIGO Scientific Collaboration, Virgo Collaboration, Fermi Gamma-Ray Burst Monitor, and INTEGRAL. Gravitational waves and gamma-rays from a binary neutron star merger: Gw170817 and grb 170817a. *The Astrophysical Journal Letters*, 848(2):L13, October 2017.

[Mei07] James D. Meiss. *Differential Dynamical Systems*. Society for Industrial and Applied Mathematics, 2007.

[NDFT10] Savvas Nesseris, Antonio De Felice, and Shinji Tsujikawa. Observational constraints on galileon cosmology. *Physical Review D*, 82(12), December 2010.

[PAG+99] S. Perlmutter, G. Aldering, G. Goldhaber, R. A. Knop, P. Nugent, P. G. Castro, S. Deustua, S. Fabbro, A. Goobar, D. E. Groom, I. M. Hook, A. G. Kim, M. Y. Kim, J. C. Lee, N. J. Nunes, R. Pain, C. R. Pennypacker, R. Quimby, C. Lidman, R. S. Ellis, M. Irwin, R. G. McMahon, P. Ruiz-Lapuente, N. Walton, B. Schaefer, B. J. Boyle, A. V. Filippenko, T. Matheson, A. S.

Fruchter, N. Panagia, H. J. M. Newberg, W. J. Couch, and The Supernova Cosmology Project. Measurements of Ω and Λ from 42 high-redshift supernovae. *The Astrophysical Journal*, 517(2):565–586, June 1999.

[PBFT19] Simone Peirone, Giampaolo Benevento, Noemi Frusciante, and Shinji Tsujikawa. Cosmological data favor galileon ghost condensate over ΛCDM. *Phys. Rev. D*, 100:063540, Sep 2019.

[PFH+18] Simone Peirone, Noemi Frusciante, Bin Hu, Marco Raveri, and Alessandra Silvestri. Do current cosmological observations rule out all covariant galileons? *Physical Review D*, 97(6), March 2018.

[PWB10] F. Pace, J.-C. Waizmann, and M. Bartelmann. Spherical collapse model in dark-energy cosmologies. *Monthly Notices of the Royal Astronomical Society*, pages no–no, July 2010.

[RFC+98] Adam G. Riess, Alexei V. Filippenko, Peter Challis, Alejandro Clocchiatti, Alan Diercks, Peter M. Garnavich, Ron L. Gilliland, Craig J. Hogan, Saurabh Jha, Robert P. Kirshner, B. Leibundgut, M. M. Phillips, David Reiss, Brian P. Schmidt, Robert A. Schommer, R. Chris Smith, J. Spyromilio, Christopher Stubbs, Nicholas B. Suntzeff, and John Tonry. Observational evidence from supernovae for an accelerating universe and a cosmological constant. *The Astronomical Journal*, 116(3):1009–1038, September 1998.

[RYM+22] Adam G. Riess, Wenlong Yuan, Lucas M. Macri, Dan Scolnic, Dillon Brout, Stefano Casertano, David O. Jones, Yukei Murakami, Gagandeep S. Anand, Louise Breuval, Thomas G. Brink, Alexei V. Filippenko, Samantha Hoffmann, Saurabh W. Jha, W. D'arcy Kenworthy, John Mackenty, Benjamin E. Stahl, and WeiKang Zheng. A comprehensive measurement of the local value of the hubble constant with 1 km s-1 mpc-1 uncertainty from the hubble space telescope and the sh0es team. *The Astrophysical Journal Letters*, 934(1):L7, July 2022.

[RZ02] S.E. Rugh and H. Zinkernagel. The quantum vacuum and the cosmological constant problem. *Studies in History and Philosophy of Science Part B: Studies in History and Philosophy of Modern Physics*, 33(4):663–705, 2002.

[Ste90] J M Stewart. Perturbations of Friedmann-Robertson-Walker cosmological models. *Classical and Quantum Gravity*, 7(7):1169, jul 1990.

[Uza11] Jean-Philippe Uzan. Varying constants, gravitation and cosmology. *Living Reviews in Relativity*, 14(1), March 2011.